

**ASSESSMENT OF HYBRIDIZATION RATIO FOR A SMALL
HYBRID-ELECTRIC BUSINESS JET**

Arailym Alibek, BEng

**Submitted in fulfillment of the requirements
for the degree of Master of Science
in Mechanical & Aerospace Engineering**



**NAZARBAYEV
UNIVERSITY**

**School of Engineering and Digital Sciences
Department of Mechanical & Aerospace Engineering
Nazarbayev University**

53 Kabanbay Batyr Avenue,
Astana, Kazakhstan, 010000

Supervisor: Associate Professor Basman Elhadidi

Co-supervisor: Professor Essam Shehab

April 2023

DECLARATION

I hereby, declare that this manuscript, entitled “*Assessment of Hybridization Ratio for a Small Hybrid-Electric Business Jet*”, is the result of my own work except for quotations and citations, which have been duly acknowledged.

I also declare that, to the best of my knowledge and belief, it has not been previously or concurrently submitted, in whole or in part, for any other degree or diploma at Nazarbayev University or any other national or intentional institution.

Name: Arailym Alibek

Date: 07.04.2023

Abstract

Within recent decades, the development of aerial vehicles with Hybrid-Electric Propulsion Systems (HEPS) has evolved into aerospace thanks to their simple incorporation of efficient powertrains. Increasing environmental concerns about traditional fuel-based propulsion systems drove major corporations to hybridize classical aircraft to minimization of CO₂, noise, and other hazardous particles by 70%. As the mission complexity among both civilian and military applications includes landing and take-off which are power-demanding, the use of hybrid-electric is necessary to overcome the deficiency of all-electric vehicles.

This thesis is primarily concerned with the development of a HEPS for a medium-range aircraft. Considered aircraft is assessed on the various hybridization ratio to estimate the optimal. Moreover, the propulsion is analyzed according to a power-based conceptual sizing methodology. During the procedure, mass distribution for five different architectures, which are all-electric, pure combustion, series, and parallel HEPS, have been simulated. For the simulation, the choice of aircraft has been chosen according to the maximum range value of more than 1000 km, which Zunum Aero ZA10 can acquire. Moreover, the thesis conducted research on three different areas of interest such as hybrid aircraft, quiet takeoff and landing, and quiet cruise target. The outcomes indicate that the hybrid design of medium-range aircraft is an optimal solution both for researchers and practitioners. Between series and parallel hybrid configurations, the comparison indicates that the latter is an ideal choice for the practitioners as it can be applied for all the considered research interest areas, whereas the series is shown as a maximum footprint reduction tool.

The thesis has contributed significantly to the knowledge of HEPS for middle-range aircraft, and the findings can be applied for the improvement of the initial performance of aircraft under specific constraints. The study has provided insights into the best ratio of fuel and battery weights for such aircraft and has compared HEPS performance in the same mission profile and speed parameters. The research has limitations, and further research is needed to combine the sizing procedure for HEPS with the actual aircraft design, explore advancements in battery and engine technology, and consider the multi-disciplinary optimization of HEPS.

Keywords: Hybrid-electric propulsion system, Zunum aircraft, Power-based sizing methodology, Propulsion configurations simulation.

Acknowledgements

I would like to express my gratitude to Professor Basman Elhadidi for his unwavering support and collaboration with the Master Thesis project. The project brings me to an exciting and at the same time challenging academic adventure, which I am happy to have been chosen to pass. Thanks to the professor, who shared hours of his time a week with me discussing aircraft performance and hybrid. This time was valuable for me to overcome the problems I had faced during the journey due to his broad knowledge of the topic, invaluable patience, and positive attitude toward an entire cycle of thesis development.

Furthermore, my research would not have been published without the assistance of Professor Essam Shehab, whose guidance brought me to the successful completion of my master's degree. His expert guidance allowed me to develop as a person and as a professional in the industry. I am glad for being chosen by you to embark on this fantastic experience and for the opportunity to further my academic career.

I am grateful to Nazarbayev University for the education I received over these years. From brilliant teachers to pleasant students, I enjoyed a fantastic atmosphere for study and collaborative growth throughout the road.

Lastly, I would like to mention my family and friends, expressing appreciation to you from the bottom of my heart. Thank you for your unending love and emotional support, which lifted my spirits when I needed it most to complete my master's degree. I am grateful to you for being an inspiring example of hard work that motivates me when my passion appears to be waning.

Thank you.

Table of Contents

Abstract.....	2
Acknowledgements	3
Table of Contents	4
List of Abbreviations & Symbols.....	6
List of Tables	7
List of Figures.....	8
Chapter 1 – Introduction	10
1.1. Motivation for Electric Aircraft Investigation	10
1.2. Literature Review	12
1.2.1. Overview of EA Classification in terms of Propulsion System.....	12
1.2.2. Advantages of Hybrid-Electric Aircraft.....	14
1.2.3. Successful cases of HEPS	15
1.2.4. Feasibility of HEPS.....	17
1.2.5. Electrification of Aircraft Propulsion System.....	17
1.2.6. Challenges in Implementing HEPS	18
1.2.7. Research Gap Analysis	20
1.3. Research Aim and Objectives	20
1.4. Thesis Layout	21
Chapter 2 – Methodology	23
2.1. Aircraft performance evaluation	23
2.2.1. Aircraft specification	23
2.2.2. Mission profile and requirements	23
2.2.3. Mission power evaluation	24
2.1.3.1. Cruise mission.....	24
2.1.3.2. Climbing and landing missions.....	26
2.2. Assessing the weight of the airframe	27
2.2.1. Initial sizing assessment.....	27
2.2.2. HEPS Assessment.....	28
2.2.3. Fuel and battery weight estimation	30
2.2.4. HEPS components' weight estimation	30

Chapter 3 – Case Study.....	32
3.1. Aircraft selection.....	32
3.1.1. Zunum Aero ZA10 specification.....	33
3.1.2. Performance representation of Zunum Aero ZA10.....	35
3.2. Simulation scenarios.....	37
3.2.1. Pure Electric and Conventional.....	37
3.2.2. Series Hybrid Electric.....	40
3.2.3. Parallel Hybrid Electric.....	43
3.2.4. Quiet Takeoff and Landing Scenario.....	45
3.2.5. Discussion.....	47
Chapter 4 – Conclusion and Future Research Directions.....	51
4.1. Conclusion.....	51
4.2. Contribution to Knowledge.....	51
4.3. Future Research Directions.....	52
References.....	53
Appendix MATLAB Code.....	57

List of Abbreviations & Symbols

HEPS	Hybrid-Electric Propulsion System
EA	Electric Aircraft
DEP	Distributed Electric Propulsion
L	Lift
T	Trust
D	Drag
c_L	coefficient of lift
c_D	coefficient of drag
q_∞	dynamic pressure
$\rho(h)$	air density at h altitude
ρ_{sL}	air density at sea level
β	constant equal to $1/9012 \text{ m}^{-1}$
AR	aspect ratio
s	span
S	wing area
c	a chord
k	variable dependent on the aspect ratio and characterizes induced drag
U_∞	mission speed, cruise, or climbing
R/C	a rate of climb
HR	hybridization ratio
ICE	Internal Combustion Engine
EM	Electric Motor
SOC	state of the charge of the battery
BSFC	brake specific fuel consumption constant
$\eta_{ICE}, \eta_{EM}, \eta_{gen}$	the efficiency of ICE/ EM or generator
P_{elec}	electric power
P_{total}	total power
$m_b, m_f, m_{ICE}, m_{EM},$ m_{gen}	mass of the battery, fuel, ICE, EM, or generator
e	a specific power of the battery
$P_{gen}^*, P_{EM}^*, P_{ICE}^*$	specific powers of a generator, EM and ICE
$P_{cruise}, P_{climb}, P_{landing}$	Powers for cruising, climbing, and landing
TO&LA	Takeoff and landing
$t_{climb}, t_{cruise}, t_{landing}$	time for climbing, cruising, and landing respectively

List of Tables

TABLE 1.1: SUMMARY OF SUCCESSFUL SMALL AND MEDIUM-SCALE AIRCRAFT	16
TABLE 3.1: THE AIRCRAFT SPECIFICATION	35
TABLE 3.2: THE AIRCRAFT CRUISE PERFORMANCE PARAMETERS	36
TABLE 3.3: POWER DISTRIBUTION DURING FULL FLIGHT MISSION, kW	36
TABLE 3.4: MASS DISTRIBUTION OF PURE ELECTRIC AND FUEL, KG	39
TABLE 3.5: MASS DISTRIBUTION OF PURE ELECTRIC, PURE FUEL, AND SERIES HEPS, KG.....	43
TABLE 3.6: MASS DISTRIBUTION OF ALL-ELECTRIC, PURE FUEL AND QUIET TAKEOFF AND LANDING HEPS ($\eta_{bat}=0.7$), KG	47
TABLE 3.7: MASS DISTRIBUTION OF ALL-ELECTRIC, PURE FUEL AND QUIET TAKEOFF AND LANDING HEPS ($\eta_{bat}=0.5$), KG	47
TABLE 3.8: MASS DISTRIBUTION OF ALL CONSIDERED PROPULSION SYSTEMS, KG	50

List of Figures

FIGURE 1.1: THE PREDICTION OF THE CARBON FOOTPRINT RISE FROM AVIATION [3]	10
FIGURE 1.2: THE PREDICTION OF THE CARBON EMISSION CONTRIBUTION OF AVIATION DEPENDS ON THE TECHNOLOGY ADVANCE BY 2050 [11]	11
FIGURE 1.3: TYPES OF ELECTRIC PROPULSION SYSTEMS FROM LEFT TO RIGHT: A) CONVENTIONAL B) ALL-ELECTRIC, C) PARALLEL HYBRID, D) SERIES HYBRID, E) TURBOELECTRIC, F) SERIES OR PARALLEL PARTIAL HYBRID, AND G) PARTIAL TURBO-ELECTRIC [12]	13
FIGURE 1.4: THE DECREASE OF THE RANGE DURING A PASSENGER CAPACITY RISE IN HYBRID AND ALL-ELECTRIC AIRCRAFT, WHOSE BATTERY`S ENERGY DENSITY IS 400-500 W H/KG [45]	19
FIGURE 1.5: PHASES OF THESIS DEVELOPMENT PRESENTED IN CHAPTERS	21
FIGURE 2.1: MISSION PROFILE SCHEME	24
FIGURE 2.2: CRUISE SPEED AND POWER RELATIONSHIP GRAPH [50].....	25
FIGURE 2.3: INITIAL MTOW SIZING TECHNIQUE [51]	28
FIGURE 2.4: SCHEME OF SERIES (A) AND PARALLEL (B) HEPS	29
FIGURE 2.5: EFFECT REPRESENTATION OF ELECTRIC OR FUEL POWER PROPORTION ON HEPS COMPONENTS MASS DISTRIBUTION	31
FIGURE 3.1: DISTANCE BETWEEN ASTANA TO ALMATY ACCORDING TO GOOGLE MAPS	32
FIGURE 3.2: ILLUSTRATION OF REFERENCE AIRCRAFT FOR ESTIMATION OF NECESSARY DIMENSIONS	34
FIGURE 3.3: POWER DISTRIBUTION GRAPH DURING FULL FLIGHT MISSION, kW VS M.....	36
FIGURE 3.4: CONVENTIONAL PROPULSION SYSTEM`S A) COMPONENTS CONNECTION B) POWER DISTRIBUTION GRAPH DURING FULL FLIGHT MISSION, kW VS H	38
FIGURE 3.5: ALL-ELECTRIC PROPULSION SYSTEM`S A) COMPONENTS CONNECTION B) POWER DISTRIBUTION GRAPH DURING FULL FLIGHT MISSION, kW VS H	38
FIGURE 3.6: SERIES HYBRID PROPULSION SYSTEM`S A) COMPONENTS CONNECTION; B) POWER DISTRIBUTION GRAPH DURING FULL FLIGHT MISSION, kW VS H; C) STATE OF THE CHARGE OF THE BATTERY DURING THE FLIGHT	40
FIGURE 3.7: SERIES HYBRID PROPULSION SYSTEM`S POWER DISTRIBUTION GRAPH FOR A) 100% AND B) 150%, kW VS H;.....	41
FIGURE 3.8: SERIES HYBRID PROPULSION SYSTEM`S STATE OF THE CHARGE OF THE BATTERY FOR BOTH 100% AND 150% OF CRUISE POWER	42
FIGURE 3.9: PROPULSION COMPONENTS MASS COMPARISON AMONG PURE ICE, ALL-ELECTRIC, AND SERIES HEPS (VARIES WITH A)	42
FIGURE 3.10: PARALLEL-1 HYBRID PROPULSION SYSTEM`S A) COMPONENTS CONNECTION; B) POWER DISTRIBUTION GRAPH DURING FULL FLIGHT MISSION, kW VS H; C) STATE OF THE CHARGE OF THE BATTERY DURING THE FLIGHT	44
FIGURE 3.11: PARALLEL-2 HYBRID PROPULSION SYSTEM`S A) COMPONENTS CONNECTION; B) POWER DISTRIBUTION GRAPH DURING FULL FLIGHT MISSION, kW VS H; C) STATE OF THE CHARGE OF THE BATTERY DURING THE FLIGHT	44
FIGURE 3.12: SERIES QUIET TAKEOFF AND LANDING SYSTEM`S A) POWER DISTRIBUTION GRAPH DURING FULL FLIGHT MISSION, kW VS H; B) STATE OF THE CHARGE OF THE BATTERY DURING THE FLIGHT	45

FIGURE 3.13: PARALLEL QUIET TAKEOFF AND LANDING SYSTEM`S A) POWER DISTRIBUTION GRAPH DURING FULL FLIGHT MISSION, kW VS H; B) STATE OF THE CHARGE OF THE BATTERY DURING THE FLIGHT	46
FIGURE 3.14: COMPARISON OF ALL-ELECTRIC, ALL ICE, SERIES, AND PARALLEL QUIET TAKEOFF AND LANDING HEPS COMPONENTS MASS PROPORTIONS (HBAT=0.7)	46
FIGURE 3.15: COMPARISON OF ALL RESEARCHED PROPULSION SYSTEMS` MASS DISTRIBUTION AMONG COMPONENTS FOR HBAT=0.7	48
FIGURE 3.16: COMPARISON OF ALL RESEARCHED PROPULSION SYSTEMS` MASS DISTRIBUTION AMONG COMPONENTS FOR HBAT=0.5	49

Chapter 1 – Introduction

1.1. Motivation for Electric Aircraft Investigation

Until these days, there was an assumption that all means of transportation will be supplied by fossil fuels to operate. However, arising environmental concerns lead to the development of solutions to reduce the negative impacts of the fuels such as climate change. The rise of the aviation industry is often regarded as the primary driver of global climate change. According to the EASA (2019), if manufacturing of fuel-based aircraft continues its production, an increase in carbon dioxide emissions is predicted to be 7 times more than it is now [1, 2]. The forecast is represented by Figure 1.1 below, where it is obvious that the growth trend of 5 percent per year will prevail for a couple of decades [3]. However, the prediction can vary according to the degree of technology development introduced in Figure 1.2 below. Moreover, from the statistical data it was established that more than 97% of aviation greenhouse gas emissions are released into the atmosphere by aircraft fuel propulsion systems [4]. In 2015 it was figured out that this conventional aircraft consumed more than 7 percent of global oil products [5]. This situation will become even worse with the increase in air fleets. Thus, the reduction of the negative impact on the environment is significantly important not only for the citizens but for all the stakeholders starting from the policy makers to aircraft designers.

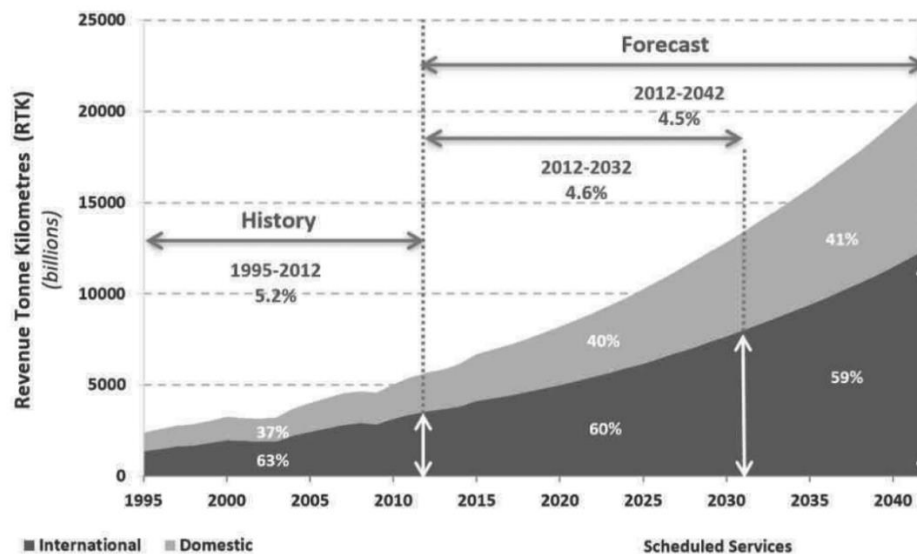


Figure 1.1: The prediction of the carbon footprint rise from aviation [3]

Consequently, this demand for a cleaner aircraft system emerged with the development of electric aircraft (EA) systems [6]. Since the early electrification of aircraft systems in the late 1990s, fuel consumption was reduced to almost 10 percent [7]. The reason for that is the partial or full replacement of propulsion systems such as pneumatic, hydraulic, or mechanical systems by electrical ones [8]. The trend of electric vehicle development is represented by the organizations such as Airbus, Boeing, NASA, and the European Commission in their future goals for 2030 and 2050. They aim to reduce CO2 emissions and fuel consumption to 75 and 70 percent respectively [9]. Another necessity of the development of EA is design simplicity, higher efficiency of power systems, the possibility of fuel-to-electric power optimization, reliability, reduction of weight, and its economic benefits [10].



Figure 1.2: The prediction of the carbon emission contribution of aviation depends on the technology advance by 2050 [11]

From the greenhouse gases model, without any development in technology the aviation will contribute to ten percent of the emissions globally compared to 25% in other industries. If the evolution of the propulsion system accelerated the participation of aviation reduces by 7%. Shifting to electrification of the aircraft reduces the degree of the emissions to 5% by 2050, however, this percentage is twice higher than today's level [11].

Literature Review

1.2.1. Overview of EA Classification in terms of Propulsion System

The propulsion systems for the electrification of aircraft are classified into three types such as hybrid-electric, all-electric, and turboelectric. In this thesis, the main consideration will be carried out by hybrid-electrical aircraft. It is necessary to note that hybrid-electric is classified as either a fully series/parallel or partially series/parallel hybrid system as compared in Figure 1.3 [12]. In a hybrid electrical aircraft, the energy is generated by jet fuel and batteries. If the thrust is obtained by a single source (combustion), then, the propulsion type is dedicated as a series. If the fan is powered by two sources (both combustion and battery), this type of propulsion is called parallel hybrid. In all the configurations of the HEPS the converters such as DC/DC are implemented to charge or discharge the battery by conversion of burnt fuel energy [13]. Nowadays, smart multiport converters are implemented rather than separate for each power port. These converters don't require multiple steps for delivering the power inside the system that improves efficiency, power density and controllability of the energy. Moreover, thanks to the galvanic isolation such converters can be integrated for different energy sources of energy as for the HEPS [14]. For aviation the most suitable power converters are recognized as triple active bridge (TAB) converters. From the research of TAB converters for different flight mission of the aircraft, it was found that they don't have energy losses during the voltage switching, however in real applications, there can be dead time, that needs to be adequate for the charging operation completion of parallel HEPS [15]. Moreover, the energy losses from high temperature are also investigated and it was found that converters have 0.25% of convection losses if they are operated under 50 °C. In addition, it was found that during the full load of the system, the efficiency of the converters is 99%, however under 50% of load, the efficiency has significantly dropped to 90% in

all considered phases such as cruising, takeoff and charging [16]. Thus, in this thesis the efficiency of the converters is neglected as the primary focus is dedicated to the components whose weight is directly relied on the power distribution of two energy sources (battery and combustion).

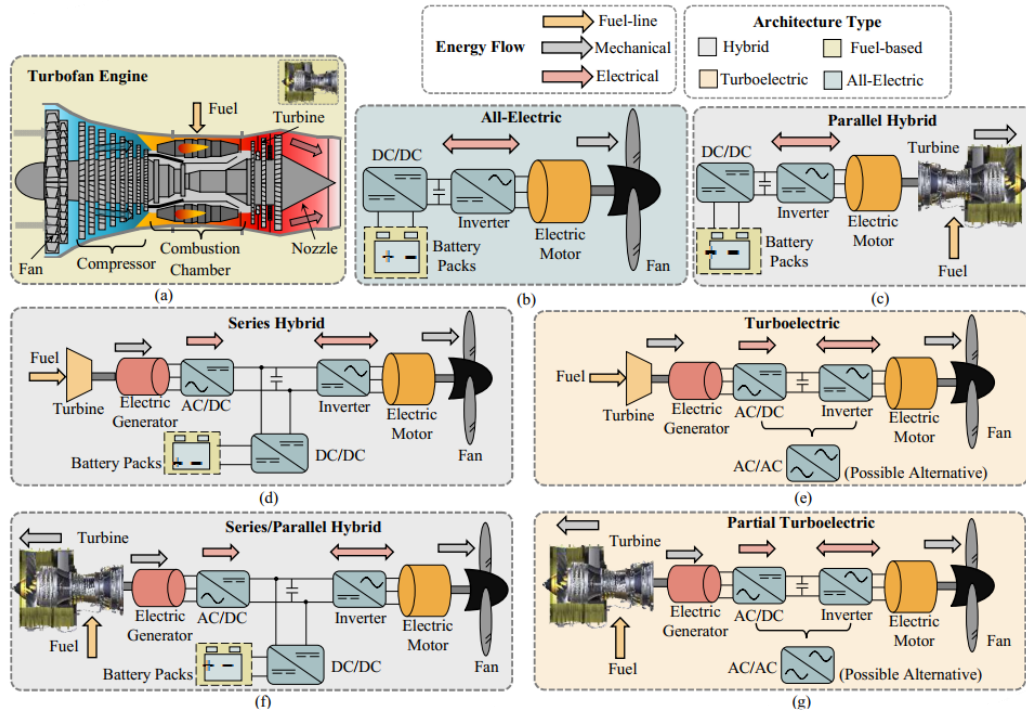


Figure 1.3: Types of electric propulsion systems from left to right: a) conventional b) all-electric, c) parallel hybrid, d) series hybrid, e) turboelectric, f) series or parallel partial hybrid, and g) partial turbo-electric [12]

Above types of electric aircraft are considered as mainly distributed among aviation industries. Another popularity is purchased by the general airplane equipped with distributed propulsion system (DEP) due to higher efficiency during the cruise and the capability to shorten the distance during the take-off and landing [17]. The concept of the DEP power system is often synergic to the previously discussed series-hybrid type where for the high-power mission the battery provides the excess power without turning off the combustion engine. However, the difference relies on the distribution of generated power to several propulsion devices (mostly fans) located along the wings or fuselage. Recognizing that it allows for vertical takeoff and landing, this kind of propulsion is frequently employed by VTOL aerial aircraft [18].

1.2.2. Advantages of Hybrid-Electric Aircraft

Initiatives to employ an electric power plant are currently being examined primarily on light jets with a take-off load of little more than 1500 kg, while for middle-scale aircraft this amount will exceed 4000 kg. This large weight of the propulsion system is not desired for today's innovations, for this reason, consideration of an all-electric case is still challenging. This is characterized by the lack of development of battery technology, which cannot achieve maturity to enable electric commercial aviation [19]. Moreover, power supply constitutes one of the most challenging components impeding the evolution of electric aircraft. The primary drawback of power supply is their relatively low efficiency, which necessitates a large weight to achieve a reasonable range and time of flight. As a result, an appealing hybrid engine is an attractive alternative between conventional and electric motors. Its use enables reduced fuel consumption, and improved service life [20].

The employment of electric motors for propulsion with either internal combustion or jet engines for power generation potentially drastically reduces overall weight while still developing innovative design concepts. A hybrid jet is built with a gas turbine power plant and a generator to power electric motors. According to different estimations, such a design will result in an airplane that uses 10% less petroleum compared to conventional aircraft. At the same time, the utilization of electric motors enables developers to drastically change the number and position of distributed motors [21].

Further features of employing hybridization innovations include a higher efficient operating mode of internal combustion engines, which is maximized by analyzing trajectories and flying patterns, in addition to the proportion of the electric power. As a consequence, the difficulties of low battery energy consumption are overcome, as well as the desired travel time and distance are delivered [22].







1.2.3. Successful cases of HEPS

Recent studies advance the development of hybrid-electric aircraft because of several benefits as increased endurance compared to all-electric. Moreover, the popularity of the hybrid is acknowledged by the significant reduction in fuel weight, emissions, and noise pollution. These advantages cause researchers to intensively work on HEPS integration to various scaled aircraft. Nowadays, the flights of small and medium scaled aircraft are successfully conducted, which proves the feasibility of HEPS application in near future.

Initially, due to the accessibility of research on small-scale aircraft systems, most academics concentrated their studies on Unmanned Aerial Vehicles (UAV). Fortunately, with an increment of awareness about the climate change causes, large aircraft organizations started funding HEPS adaptability studies for heavier aircraft. Firstly, the University of Cambridge introduces the SOUL aircraft which was believed to be the first parallel hybrid airplane demonstration[23], whereas the DA-36 has been considered the first series HEPS. From two of these aircraft, the development of HEPS was claimed to improve the range and endurance characteristics of the reference airplanes and applied to larger types [24].

In 2019, Ampaire tested the EEL, which replaced the conventional Cessna 337 aircraft. In this aircraft, the total decoupling of ICE and EM has been conducted, which limited the HEPS to charge the battery during the flight [25]. HEPS application is also applied to helicopter-like aircraft that have the capability to vertically takeoff from the ground and land (VTOL). For these aircraft, the distributed electric motors are implemented and powered by the single gas turbine engine as for the eVTOL constructed by Rolls-Royce [26]. Earlier, the first VTOL concept was experienced by the Workhorse group in 2018. Their aircraft called Surefly had lower propulsion efficiency which causes a decrease in its speed and range performance [27]. The summary of all these aircraft systems is described in Table 1.1.

Table 1.1: Summary of successful small and medium-scale aircraft

№	Aircraft	Name	Organization	Hybrid architecture	MTOW, kg	Power, kW
1		SOUL	UC, Boeing	parallel	210	12
2		Electric EEL	Ampaire	parallel	2100	180
3		EVTOL	Rolls-Royce	series/ parallel	450	500 - 1200
4		Eco Caravan	Magnix, SurfAir	series/ parallel	1130	560
5		Surefly	Workhorse	series	680	150
6		DA36 E-Star	Dimond, Siemens	series	770	70

1.2.4. Feasibility of HEPS

Recent studies in the field of HEP consider comprehensive review works on how feasible its application is in near future from commercial and general aviation aircraft to regional aircraft [28-31]. Next important pieces of research apply range equations for solving the aerodynamic performance models of HEP for a particular mission type [32, 33]. Most of these studies assume that the constant amount of fuel is consumed independently of flight characteristics such as speed and altitude even though they are considering electrification of HEP where the mission is changed timely [34]. All these works have been focusing on the various effects of batteries, aircraft design configurations, and hybrid propulsion systems on mission performance. They often neglect effects from the flight characteristics such as flight altitude and flight speed changed by time, which is crucial in evaluating the feasibility of HEP. The reason for that could be the necessity of multidisciplinary knowledge, where the HEPS optimized taking into account all the contributing factors such as the sizing of all main components, energy sources related to the flight mission, programming logical energy management system, and sizing of power electronics and cooling systems, whose weights can be significant to be neglected [35].

1.2.5. Electrification of Aircraft Propulsion System

One of the first proposals for the electrification of conventional fuel-based aircraft was obtained by extending the conventional sizing methodology [36]. The extension was conducted by applying the hybrid retrofit concept. The findings from the comparison of the conventional and modified aircraft show that during short flights, electrification saved almost 20 percent of fuel. The same findings can be seen from a similar mission flight, skydiving [37]. Skydiver lift requires high power even though its duration is short. This study introduced that HEPS can guarantee powerful performance at the same time reducing the weight of fuel and CO₂ emissions. Knowing the advantage of electrification, researchers proposed an integrated sizing methodology to examine aspects of influence [38, 39]. They have found that consideration of the mission and power profiles of the aircraft is crucial in meeting requirements of take-off performance. During the procedure, the weight of the aircraft could be minimized, which proved the advantage of implementing HEPS.

To indicate that the middle-scale hybrid-electric jets are a great compromise for both researchers and manufacturers, a comprehensive review of the literature starting from UAVs to commercial aircraft was carried out [40]. The propulsion hybridization of middle-scale aircraft is the most ideal problem to investigate because there is enough battery power for large aircraft, which waits for their evolutionary improvement. Moreover, it was found that UAV is the most studied topic due to its easy implementation, which loses the interest of the researchers. Thus, the next studies will be reviewed for the same class of aircraft hybridization. The first research was conducted on the evaluation of the performance of the Cessna 337 propulsion system [41]. The constraints of the research have been chosen to have the same MTOW and mission and compare three electric configurations with the conventional benchmark. Electric configurations have been chosen to be all-electric, series, and parallel hybrid for their investigation during preliminary design. It has been found that parallel hybrid electric propulsion is an advantageous option in terms of savings of emission release and energy consumption.

1.2.6. Challenges in Implementing HEPS

Adapting the hybrid electrical power system for the airplane is an ambitious goal due to technical deficiencies. The major issue is associated with the technological advancement of batteries. Due to poor specific energy (at most 300Wh per kilogram) and temperature instability, contemporary battery packs are not compatible with use in airplanes for commercial use. As opposed to a kilogram of kerosene, storing energy in 12.4 kg leads the system to be overweight. Moreover, current batteries reduce the endurance of the aircraft to 20 min, for achieving an hour of this flight time the specific value of the battery needs to be doubled [42]. In addition, to handle temperature destabilization, a complex system of cooling and temperature control must be evolved into HEPS [43].

Even though hybrid-electrical aircraft is a great compromise between conventional and electric propulsion systems, it is still depending on energy storage systems. The main parameters needed for the determination of an aircraft's flight range and carried payload are densities of energy and power [44]. Higher power is consumed by aircraft during the takeoff and climb missions. Thus, at a longer range of flight, the power is not enough for carrying a larger number of passengers, which is described by state-of-the-art batteries as represented in Figure 1.4 [45].

This relationship between range and payload demonstrates a significant disadvantage compared to fuel-based systems. Thus, this research project will investigate the optimal degree of hybridization to increase the payload capacity on a constant aircraft range (over 1120 km). As seen from the figure below, for this given range, only hybrid-electric vehicles are suitable. Moreover, the considered problem will assess only for the business jets class.

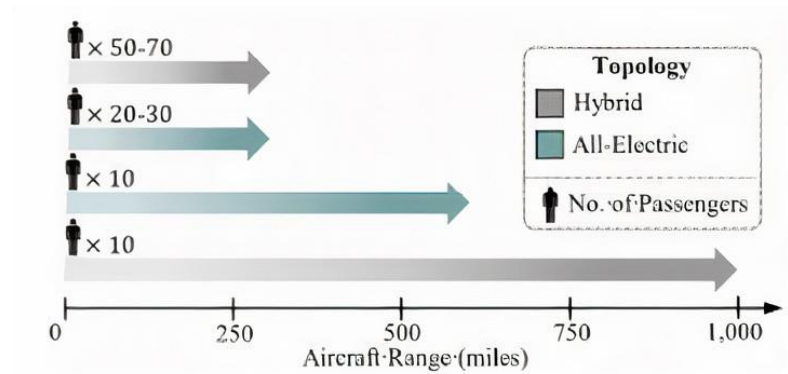


Figure 1.4: The decrease of the range during a passenger capacity rise in hybrid and all-electric aircraft, whose battery's energy density is 400-500 Wh/kg [45]

There are also other challenges that are equally important in determining the feasibility of the overall system, such as reliability, life cycle, and cost of each powertrain component. The main components, including electric machines, power converters, and battery packs, must meet strict safety and reliability standards specific to the aerospace industry, such as DO-254 [46]. Moreover, current lifetime models for these components may need modifications to be applicable in aerospace conditions. Therefore, addressing reliability and life cycle requirements is critical. On the other hand, cost is a secondary priority influenced by the scalability business models of the aerospace industry [47].

In terms of safety considerations, due to a lack of adaptability of electrical installations for the higher altitude of the aircraft operations, there is a risk of system's reliability as the system operates at a high power that requires high voltage and currents. Frequently, this risk is tested on the ground and initial insulation issues of aircraft materials have been identified and tackled. It has been observed that when creating high voltage components, it is crucial to take extensive precautions to prevent the leakage of the high voltage network into the low voltage network. This

low voltage network facilitates the communication and power supply of the control elements in the system and the aircraft in an integrated system. If this leakage is not adequately contained, it can result in the failure of critical aircraft systems. Therefore, it is important to prevent such leakage to ensure the safety and reliability of the overall system [48].

1.2.7. Research Gap Analysis

During the analysis of the literature review, several gaps have been identified:

1. Combined consideration of the parameters of the airframe, propulsion system, and flight conditions is crucial in assessing the full potential of HEP [35]. Thus, optimization of all three parameters is necessary for the improvement of HEP's overall performance.
2. There is a lack of study that compares the performance of all three types of HEP for regional (business) aircraft systems.
3. A few studies investigated the fuel-saving potential of HEP for simple missions and not complete flight in describing take-off, cruise, and landing.
4. Further testing of existing batteries needs to be carried out to determine the capacity reduction during recharging and battery degradation.
5. The results of the experimental work conducted for a specific type of HEP indicated the importance of further research on the relationship between fuel saving and battery life in order to optimize their performance [49].

1.3. Research Aim and Objectives

The primary aim of the thesis is to assess the hybridization ratio for a medium-range business aircraft. This aim helps to evaluate if HEPS is a feasible solution for business jets. The objectives are:

1. To investigate the payload excess of the considered aircraft's propulsion system under simulation of five considered scenarios.
2. To assess the reference aircraft's power supply strategy for series, parallel HEPS, all-electric, all ICE, and for quiet takeoff and landing scenarios.

- To establish the optimal hybridization ratio after acquiring the weight distribution of hybrid-electric energy sources for series and parallel HEPS.

The evaluation of the HEPS for the business jet will be developed on the MATLAB® framework. This framework has the potential for a power-based sizing method as the work will quantitatively assess different aircraft propulsion configurations. This thesis will allow to designers identify design alternatives according to the specific requirements.

1.4. Thesis Layout

The thesis will be systemized and organized into appropriate chapters presented in Figure 1.5 below.

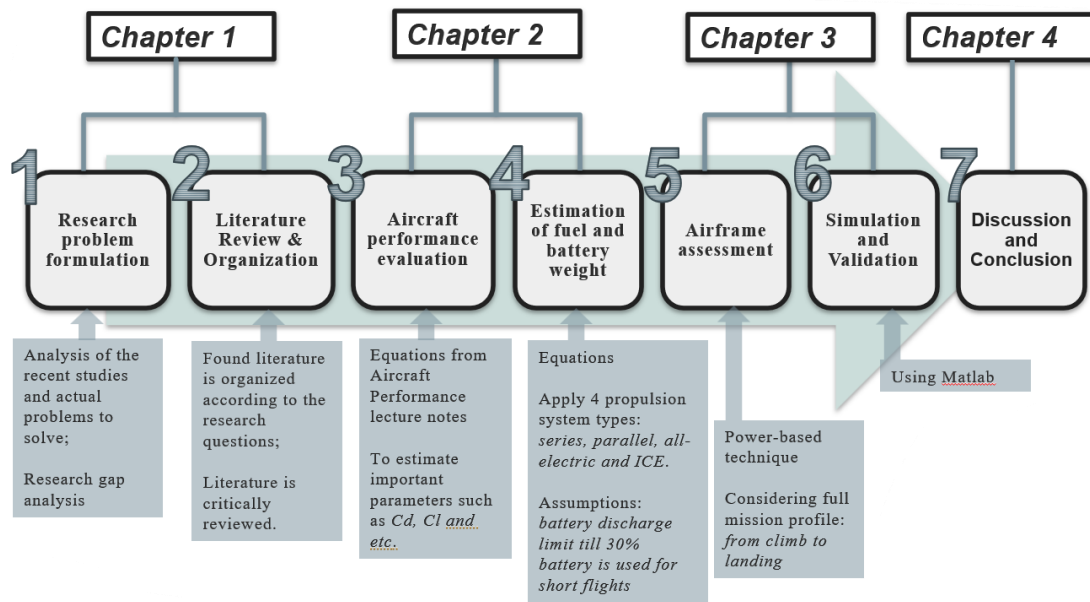


Figure 1.5: Phases of thesis development presented in chapters

Chapter 1 introduces the motivation behind zero-emission aircraft development and justifies the electric modification of the propulsion systems of the aircraft. In the literature review section, the concise revision of the latest research publications is introduced and critically analyzed to determine the research gaps. Moreover, Literature Review presents the background of the problem and covers the description of the EA and various configurations of aircraft propulsion. Finally, the main goal of the thesis is introduced which is outlined.

Chapter 2 will cover a theoretical overview of the aircraft's performance characterized by the mission profile. This chapter presents the working principle and the sizing techniques of primary components of HEPS according to the change of electrical power proportion in series and parallel configurations.

The simulation framework is presented in *Chapter 3*. The numerical models for the hybrid series, hybrid parallel, quiet takeoff and landing, and quiet target (military missions) are presented and explained with the acquired results to compare all the propulsion systems against a conventional one.

Lastly, the conclusion is discussed in *Chapter 4*. This chapter completes the thesis presenting HEPS design for future applications. Moreover, there a rational preference for one of HEPS is estimated to fulfill most of the research interests.

Chapter 2 – Methodology

2.1. Aircraft performance evaluation

Aircraft performance needs to be evaluated to estimate the power capabilities of the aircraft in different flight missions and durations. Due to the consideration of the full mission profile, the thesis will cover the research gap of both short and long missions. Moreover, the thesis will analyze the full mission profile covering climbing, cruising, and landing. Specific aircraft are under analysis to estimate the mass distribution of propulsion components, fuel, and battery. All estimated data are needed to quantitatively assess the proposed design.

2.2.1. Aircraft specification

For the performance evaluation, the primary aircraft specifications need to be determined from the open sources provided by the manufacturer. The main parameter of the aircraft is always considered in terms of an AR that has a direct effect on the lift and drag forces. Knowing the dimensions of the reference aspect ratio were calculated using the wing geometry approach and presented below as equation 2.1. The reference aircraft dimensions are presented in Table 3.1, which was calculated using the given two-dimensional drawing from the manufacturer presented in Figure 3.2 in the next chapter.

$$AR = \frac{s}{c} = \frac{s^2}{S} \quad (2.1)$$

where, AR is the aspect ratio, s – span, S – wing area and c is a chord.

2.2.2. Mission profile and requirements

During the research, the mission profile is simplified as the climb – cruise – landing phases as the primary focus here is to assess the propulsion system. The RC for takeoff and landing missions is illustrated for the reference model by Zunum. The schematic view of the mission profile is seen in Figure 2.1. During landing the power requirements can be reduced by cutting back power for the engines and gliding, however, this scenario is not considered as it is only possible in good weather. Here powered landing is considered.

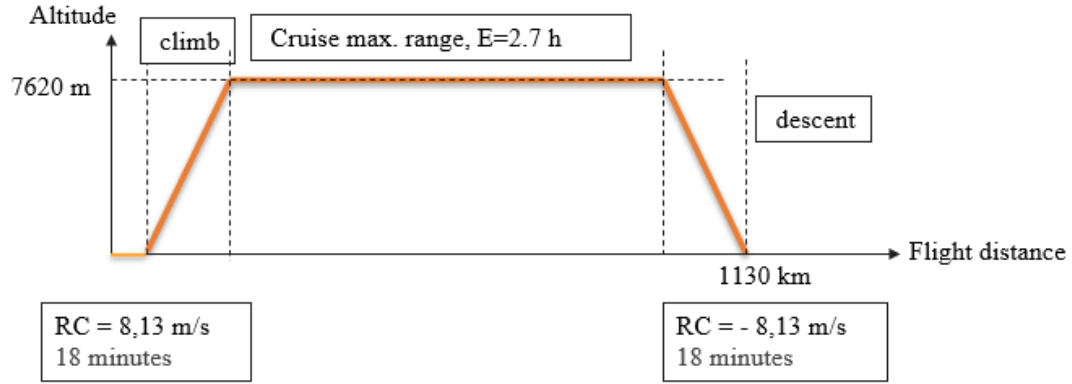


Figure 2.1: Mission profile scheme

The requirement to successfully complete the mission is to maintain the maximum range and endurance even after the hybridization of the aircraft. Moreover, the payload mass needs to be more than it is designed. The last requirement is aimed to be satisfied by the reduction of fuel mass and is discussed in the “initial sizing assessment” section. Lastly, the MTOW of the aircraft needs to be equal to the initial MTOW.

2.2.3. Mission power evaluation

2.1.3.1. Cruise mission

During the constant altitude flight as cruise, lift and drag equations are given by

$$L = W = q_{\infty} S c_L \quad (2.2)$$

$$D = T = q_{\infty} S c_D = q_{\infty} S (c_{Dmin} + k c_L^2) \quad (2.3)$$

where k is a variable dependent on the aspect ratio and characterizes induced drag, $k = \frac{1}{e\pi AR}$,

L is a lift, D – drag, T is a thrust force, c_L and c_D are the coefficients of respective forces such as lift and drag, W here assumed equal to the difference of MTOW and half fuel mass, q_{∞} is a dynamic pressure, which is characterized as

$$q_{\infty} = \frac{\rho(h)v^2}{2} \quad (2.4)$$

where v is cruise velocity, $\rho(h)$ is air density at h altitude, which is calculated by $\rho(h) = \rho_{SL}e^{-\beta h}$, using density at sea level (ρ_{SL}) and β is a constant = $1/9012 \text{ m}^{-1}$.

Knowing the cruise speed, the coefficient of lift can be estimated, however coefficient of drag remains unknown. The relationship between power and velocity is presented in Figure 2.2.

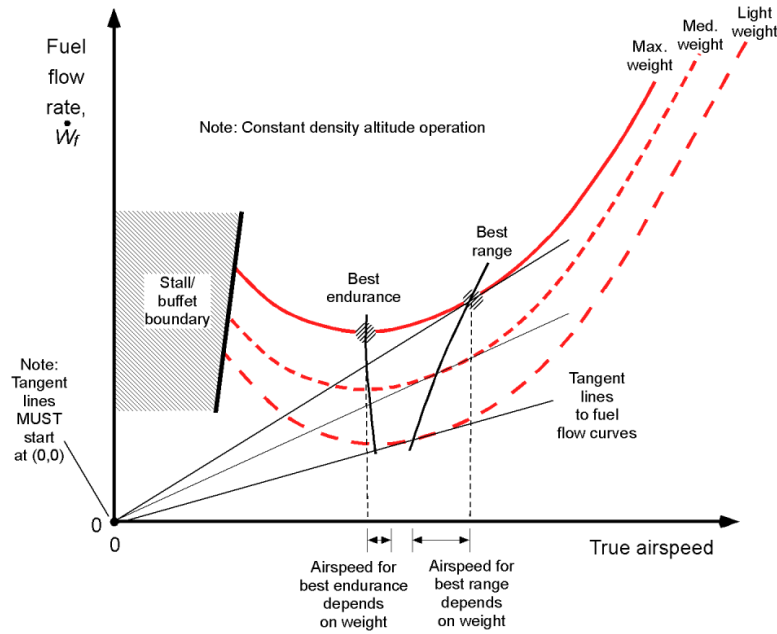


Figure 2.2: Cruise speed and power relationship graph [50]

From the figure, it is seen that at the minimum power speed, where the maximum range of the flight can be acquired, the coefficient of drag is equal to the multiplication of the minimum coefficient of drag twice. At this point (at the point where the ratio of lift to drag is maximum) cruise velocity can be calculated from

$$U = \sqrt{\frac{2}{\rho} \left(\frac{W}{S} \right) \sqrt{\frac{k}{c_{D_{\min}}}}} \quad (2.5)$$

Moreover, the minimum coefficient of drag can be calculated from the known economy cruise velocity, where the maximum endurance (at $c_L^{3/2} / c_D$) can be estimated by

$$U = \sqrt{\frac{2}{\rho} \left(\frac{W}{S}\right) \sqrt{\frac{k}{3c_{D_{\min}}}}} \quad (2.6)$$

The power required for the completion of the cruise mission is calculated from the general formula below

$$P_R = T U_\infty \quad (2.7)$$

where U_∞ is a cruise speed.

2.1.3.2. Climbing and landing missions

During the climbing, there is excess power is generated as the value of the trust force is much higher than the drag

$$(T - D)U_\infty = W R/C \quad (2.8)$$

where W is equal to MTOW, R/C is the rate of climb and U_∞ is equal to climbing velocity. For landing, the equation above is modified and excess power become

$$(T - D)U_\infty = (W - W_f) R/C \quad (2.9)$$

where W is equal to MTOW, W_f – is the weight of consumed fuel, and U_∞ is equal to landing velocity. The whole power for completion of landing and climbing missions can be calculated by

$$P = \frac{1}{2} \rho U^3 S c_D \pm \text{Excess Power} \quad (2.10)$$

where U corresponds to climbing or landing velocities.

2.2. Assessing the weight of the airframe

After the calculation of how much power is needed for the different missions, the values are used for the estimation of the total power needed for the aircraft's successful operation. Assessment of the airframe is conducted for the comparison of fuel weight and battery weight in different propulsion systems. The considered powertrains are all-electric, purely fuel, series, and parallel hybrid electric.

2.2.1. Initial sizing assessment

Initial sizing assessment is a traditional technique to analyze the change of MTOW of the aircraft [51]. MTOW is estimated from the sum of empty aircraft mass, the mass of fuel and battery, and payload mass and is defined below

$$MTOW = m_{empty} + m_{fuel} + m_{battery} + m_{payload} \quad (2.11)$$

All these values of weight, except payload mass, are considered variables and calculated for four considered propulsion systems. Weight of fuel and battery estimated for each flight mission starting from climbing to landing. Empty mass considers the mass of the internal combustion engine, generator, and electric motor, which will be described in the "HEPS components evaluation" section.

After the calculation of modified HEPS masses, the new MTOW is estimated and compared with the initial MTOW. If the new is larger than the initial, the sizing is repeated until it reaches the lower value. The process of this traditional method is introduced in Figure 2.3 below.

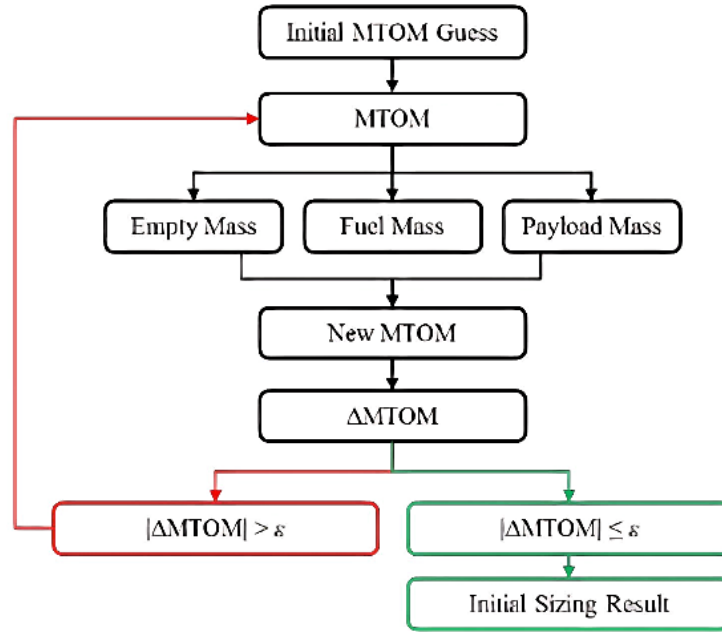


Figure 2.3: Initial MTOW sizing technique [51]

2.2.2. HEPS Assessment

The value of electrification of the propulsion system is defined from the hybridization ratio. This important index allows us to classify HEPS by the proportion of electrical power of its total power consumed, which is defined using the following formula:

$$HR = \frac{P_{elec}}{P_{total}} \quad (2.12)$$

In this thesis, the hybridization ratio varies with the change in the value of electric power (P_{elec}) to investigate the optimal proportion that guarantees the successful completion of the aircraft's full mission profile.

Hybridization of the considered aircraft can be arranged as a series or parallel. The advantages and disadvantages of these propulsion systems are described in the “Literature Review” section. In this section, the power supply control would be discussed according to the flight mission. The change of HEPS’s elements according to the type of power supply is indicated in Figure 2.4 guided with different colors.

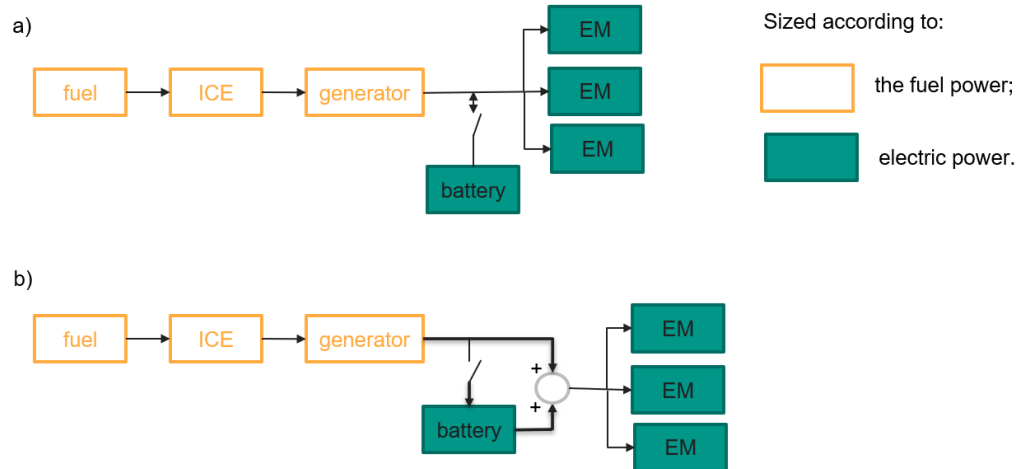


Figure 2.4: Scheme of series (a) and parallel (b) HEPS

General assumptions applicable for all propulsion types under simulation:

1. As ideal case, the battery can be consumed only till 30% is left. This is needed to overcome unpleasant situations such as heating the battery and so on. Moreover, the comparison of rough values such as 30% and 50% of left battery power will be provided as it is known that the latter is mostly assumed in the automobile industry [52].
2. The battery will be used for short-flight missions such as climbing and landing to save the fuel burnt.
3. Charging of the battery will be held only during the cruise mission.
4. At cruise, fuel is used for charging the battery and for mission performance.

In terms of energy control of series HEPS, due to the fact that only one source of energy can be used at a time, the only battery will be used during short-duration missions. On cruise flights, only fuel will be consumed to power the battery and complete the mission. The DEP can be additionally applied to series HEPS.

In the application of the parallel HEPS, both electrical and mechanical energies can be consumed at the same time. Thus, the excess power during climbing and landing will be supplied by the battery, while energy from the fuel goes to the remaining power. Moreover, during the cruise battery will be charged with two options either slowly charging the entire cruise time or fast charging several times during the cruise flight. However, the DEP cannot be allowed in the parallel configuration.

2.2.3. Fuel and battery weight estimation

The weight of the fuel is estimated by brake specific fuel consumption constant, which is characterized by BSFC, thus, the efficiency of the engine is used in the formula below

$$m_f = \frac{BSFC}{\eta_{ICE}} \times P_{ICE} \times t \quad (2.13)$$

where BSFC = 225 g/kWh for gasoline [53], which is mostly used in aircraft, t is the corresponding mission time, η_{ICE} – internal combustion engine efficiency.

Battery mass estimation is conducted by the equation below,

$$m_b = \frac{P_{EM} \times t \times \frac{1}{\eta_{bat}}}{e} \quad (2.14)$$

where η_{bat} is efficiency of the battery assumed as 0.7 or 0.5 as it has a discharge limit (not less than 30% and 50% of the battery should be left in the bank). e is a specific power of the battery that is chosen as 250 Wh/kg, which corresponds to the Li-ion batteries [53]. The formula above (2.14 and 2.15) are presented as a general to represent the relationship of the power to the masses of the energy sources and HEPS components such as electric motor, generator, and ICE. The formulas for the last three components will be presented in the next section.

2.2.4. HEPS components' weight estimation

During either parallel or series configuration, the ICE and generator are sized according to the required power supplied from fuel, while the battery is sized dependent on the electrified power. For series HEPS, ICE can operate at the optimum efficiency, thus ICE is typically sized to meet the average power demand, whereas the electric motor and battery are supplied at the maximum power. The change of power proportion during the full mission profile gained from either fuel or battery will affect the size of HEPS components, battery weight, and fuel mass, which is clear from Figure 2.5.

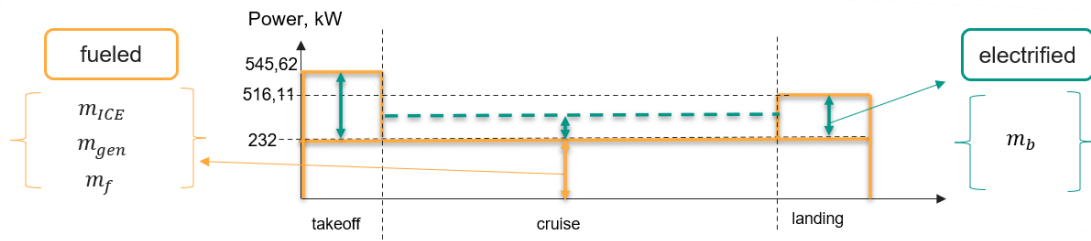


Figure 2.5: Effect representation of electric or fuel power proportion on HEPS components mass distribution

The mass distribution of the components is calculated by a set of equations (2.15) below

$$\begin{aligned}
 m_{ICE} &= \frac{P_{ICE}}{P_{ICE}^* \eta_{ICE}} \\
 m_{EM} &= \frac{P}{P_{EM}^* \eta_{EM}} \\
 m_{gen} &= \frac{P_{ICE}}{P_{gen}^* \eta_{gen}}
 \end{aligned}
 \tag{2.15}$$

where m_{ICE} , m_{EM} and m_{gen} are the masses of the internal combustion engine, electric motor, and generator respectively. Specific powers of the generator (P_{gen}^*) and electric motor (P_{EM}^*) are similar and equal to 5 kW/kg, whereas the power of ICE P_{ICE}^* is 1 kW/kg.

Chapter 3 – Case Study

3.1. Aircraft selection

The aircraft is selected according to the desired range of the flight which is chosen to be above 1000 km as the main business routes between large cities are dedicated to the considered range such as the distance between Almaty and Astana in Kazakhstan (973 km).

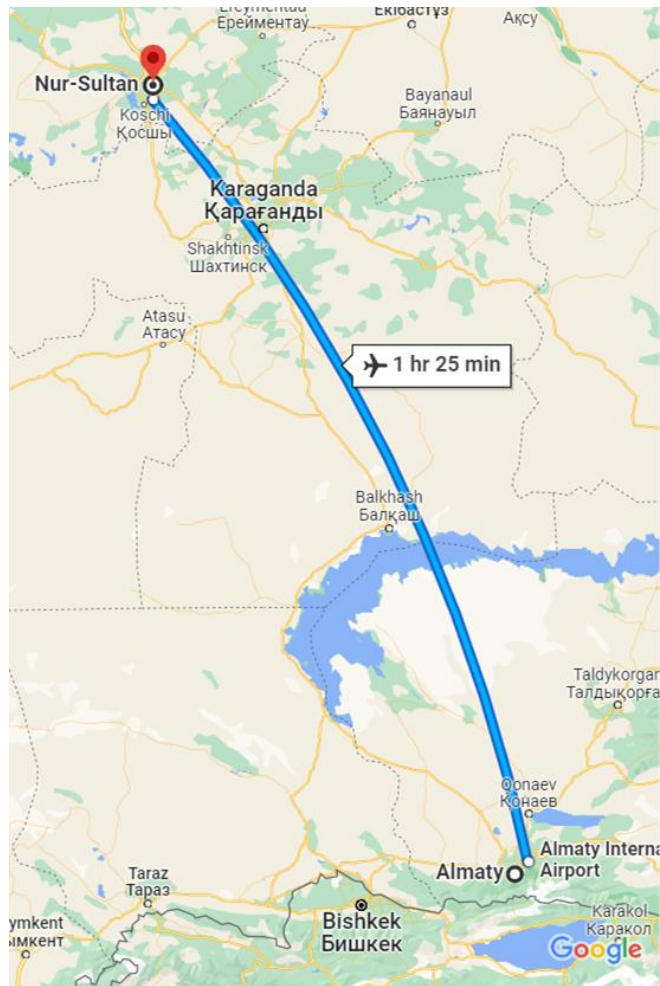


Figure 3.1: Distance between Astana to Almaty according to Google Maps

Only one business jet could satisfy the range requirement. For this reason, Zunum Aero ZA10 has been selected as a reference aircraft for the research. Next, the aircraft's specifications are collected and analyzed under the case study.

3.1.1. Zunum Aero ZA10 specification

For the electrification of the aircraft and its comparison with the conventional one, the model aircraft has been chosen. The middle-scale aircraft called Zunum Aero ZA10 was able to satisfy initial requirements such as a range not less than 1000 km and the type of aircraft to be a business jet. Zunum Aero started to design the aircraft at the end of 2017 in partnership with Boeing [54]. The first testing of the aircraft performed three years later and its delivery to the world was scheduled for this year.

ZA10 was designed for the regional airliner in Washington in order to reduce operating costs by more than 60 percent. This was done by increasing the number of passengers on board, where the six in VIP, nine in premium, and 12 in economy class, which contributes to the operating cost of the plane as 250 dollars/hour. The total number of passengers including crew members is equal to 27.

Another influence on the operating cost reduction is the aircraft's electrification. The technology of ZA10 is designed as a modification of the conventional Rockwell Turbo Commander, whose specific parameters are applied as reference values such as range, MTOW, and cruise speeds. All the specifications are written in Table 3.1 below.

For the estimation of the aircraft's wing dimensions the reverse engineering technique was applied. For this reason, the aircraft's drawing provided by the manufacturer was printed to estimate the scale of the picture. Afterward, it makes us possible to estimate the nearly exact value of the chord of the wing to determine other necessary values such as AR and S. The drawing is represented in Figure 3.2.



Figure 3.2: Illustration of reference aircraft for estimation of necessary dimensions

The powertrain of the ZA10 consists of a turboshaft engine from the Safran company, which has almost 2000 horsepower. This engine actually was developed for the helicopter and then modified for the ZA10 and became Ardiden 3Z. For feeding two electric fans, whose power is half Mega Watt, a similarly powered generator is implemented. However, there is no information about the battery applied for the given aircraft system, but there is data that battery weight is required to be less than twenty percent of its MTOW.

Table 3.1: The aircraft specification

Specification	SI unit	
<i>Weight distribution</i>		
MTOW	5215	kg
fuel weight	363	kg
max. battery weight	782,25	kg
empty weight	3720	kg
<i>Dimensions</i>		
length	13	m
span	16	m
chord	1,44444	m
aspect ratio	11,1111	
wing area	23,04	m ²
<i>Cruise performance parameters</i>		
normal cruise speed	142	m/s
economy cruise speed	117	m/s
max. cruise speed	152	m/s
cruise altitude	7620	m
density @cruise	0,53	kg/m ³
<i>Powertrain</i>		
turbo-generator	500000	W
electric fan *2	1000000	W
electric engine	1000000	W

3.1.2. Performance representation of Zunum Aero ZA10

Representing the performance of the considered aircraft is a crucial part of the thesis, where each mission of the flight is characterized by the power, time of the flight, and speed distribution necessary to achieve the primary aim of the project. Using the performance data in Table 3.1 and equations defining c_L , c_D and U_{cruise} for maximum range and endurance, the specifications of the plane are:

Table 3.2: The aircraft cruise performance parameters

c_L	c_D (max. endurance)	c_{Dmin}	c_D (max. range)	L/D	T [N]	P_R [kW]
0.4024	0.0133	0.0066	0.0133	30.2769	1633	232

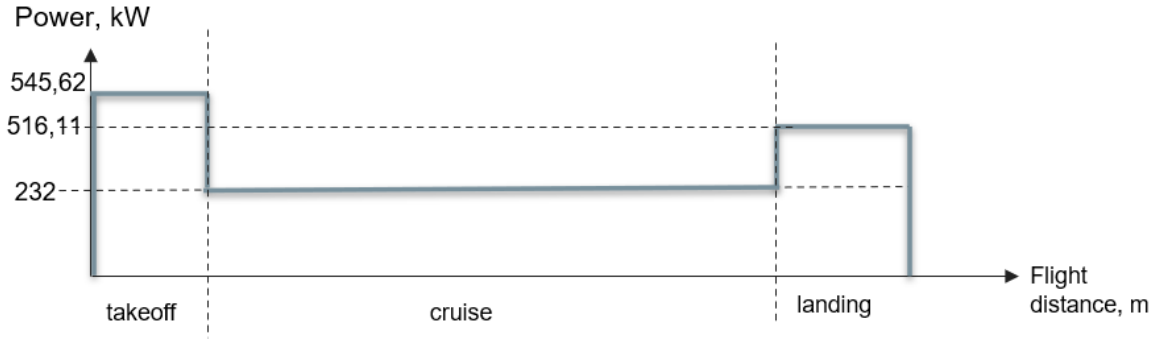


Figure 3.3: Power distribution graph during full flight mission, kW vs m

Table 3.3: Power distribution during full flight mission, kW

P_{cruise}	excess P_{climb}	P_{climb}	excess $P_{landing}$	$P_{landing}$
232	325.78	545.62	296.27	516.11

3.2. Simulation scenarios

The modeling approaches programmed in MATLAB® to simulate the performance of the propulsion components are described in this chapter. The primary goal of this study is to enhance the framework's capabilities to satisfy the requirements of multiple architectures and airframe configurations. To enable more complicated distributed propulsion systems instead of individual propeller ones, a multivariable method is used. The sizing of the elements serves as a main driver towards allowing for more exploration of all the potential combinations in designing HEPS. The sizing of the elements and energy sources such as fuel and battery will be combined according to the four simulation scenarios described in the next sections.

As a reference, firstly, the scenarios for the pure electric and conventional propulsion systems need to be presented for the comparison of their data with the research interest areas: series, parallel, quiet takeoff and landing, and quiet target.

3.2.1. Pure Electric and Conventional

Firstly, the conventional propulsion system is introduced to present which of its components are sized according to the power generated from fuel. The schematic presentation of the propulsion system is clear in Figure 3.4a below. The scheme represents the flow of the energy and its transformation among the propulsion frameworks. The next graph, figure 3.4b, represents the proportion of the power that is generated here by the fuel (described by the power-based sizing method).

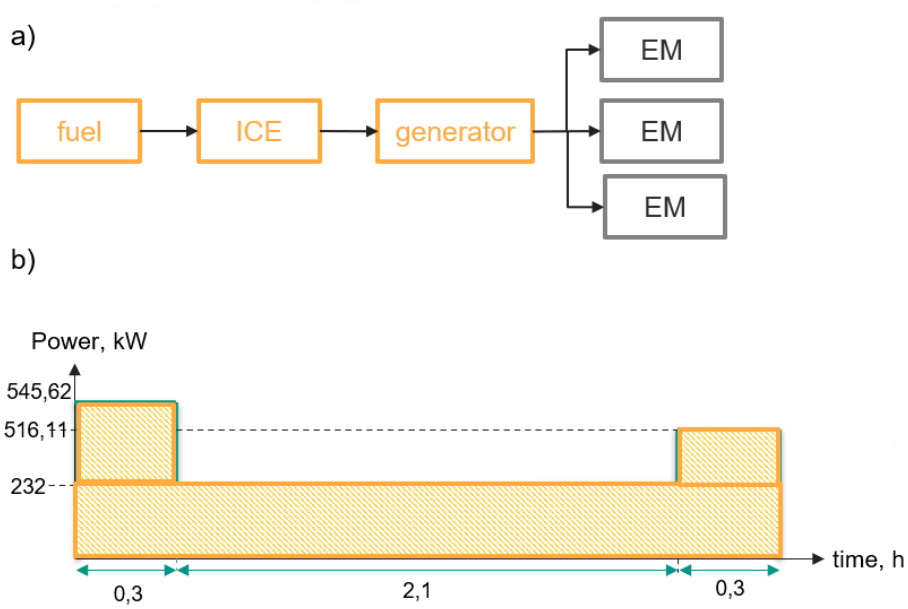


Figure 3.4: Conventional propulsion system`s a) components connection b) power distribution graph during full flight mission, kW vs h

Similarly, the same sizing of the power is conducted to the pure electric configuration to represent how the propulsion is modified and power is distributed. The simulation of the all-electric case is presented in Figure 3.5.

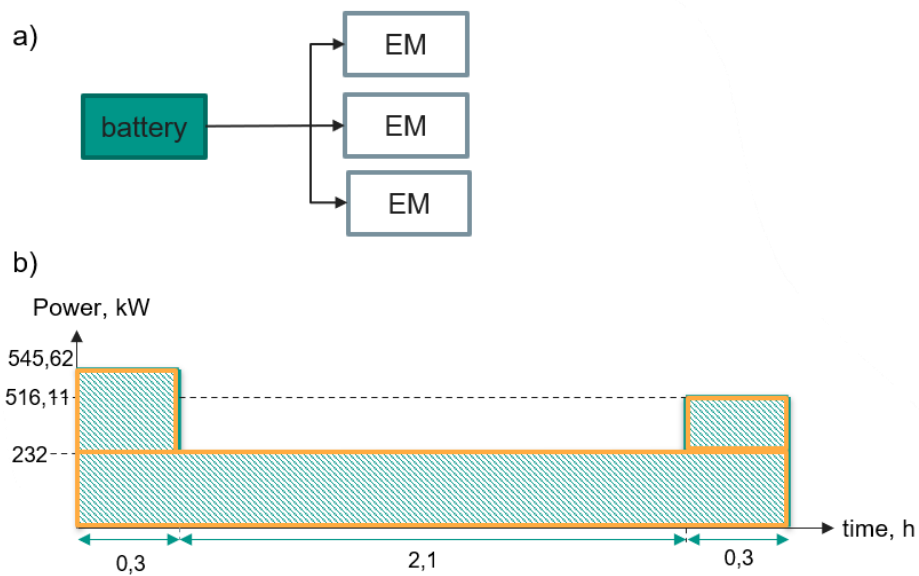


Figure 3.5: All-electric propulsion system`s a) components connection b) power distribution graph during full flight mission, kW vs h

The equation (3.1) for the mass of fuel for the former configuration and the mass of battery for the latter configurations are modified as followings:

$$m_f = \frac{BSFC}{\eta_{ICE}} \times (P_{climb} t_{climb} + P_{cruise} t_{cruise} + P_{landing} t_{landing});$$

$$m_b = \frac{1}{\eta_{bat}} \left(\frac{P_{climb} t_{climb} + P_{cruise} t_{cruise} + P_{landing} t_{landing}}{e} \right)$$
(3.1)

Table 3.4 compares the weight distribution between two propulsion configurations. From the comparison, it is obvious that the mass of the electric motor remains unchanged as for both of the propulsion types the outcome power does not differ even though the weight of the aircraft is affected.

Table 3.4: Mass distribution of pure electric and fuel, kg

Components	Conventional	All-electric ($\eta_{bat} = 0.7$)	All-electric ($\eta_{bat} = 0.5$)
EM	104	104	104
Battery	-	4 202	5 883
Generator	104	-	
ICE	212.2	-	
Fuel	413.6	-	
total	833.8	4 306	5 987

Moreover, comparing the two configurations the limitation of the all-electric propulsion system is discovered. Since an increase in propulsion mass causes decreases in payload twice, the application of the latter propulsion will be limited in the efficiency of either passenger transportation or cargo missions.

By the combination of the components in both previous systems, the propulsion leads to a hybrid modification. The modified propulsion system differs from each other in the way of components' connection with each other and the ability to power an electric motor with one source of power or two combined. Their difference is fully described in Chapter 2.

3.2.2. Series Hybrid Electric

The propulsion system of the series hybrid connects the components for acquiring all the power from the fuel to run the electric motor. Excess power can be provided from the battery capacity only for the climbing and landing missions, which requires a significant amount of power. The sizing of the elements according to the type of energy source used can be analyzed in Figure 3.6a, b. With the guidance of the color, it became understandable that the weight of the fuel, ICE, and generator is sized according to the ICE power, whereas the battery mass depends on the proportion of electrified power inside the propulsion system. Only EM has a constant value as it is discovered to depend on the total power value, which does not change by the thesis requirements. Consumption of the battery is introduced in Figure 3.6c to illustrate when the battery is turned on and how fast it is discharged. The propulsion effectiveness is evaluated according to the key parameters such as state of the charge of the battery and mass of the fuel consumption during the mission flight. During the preliminary design stage, the expected results under the system's requirement is discussed for these two parameters.

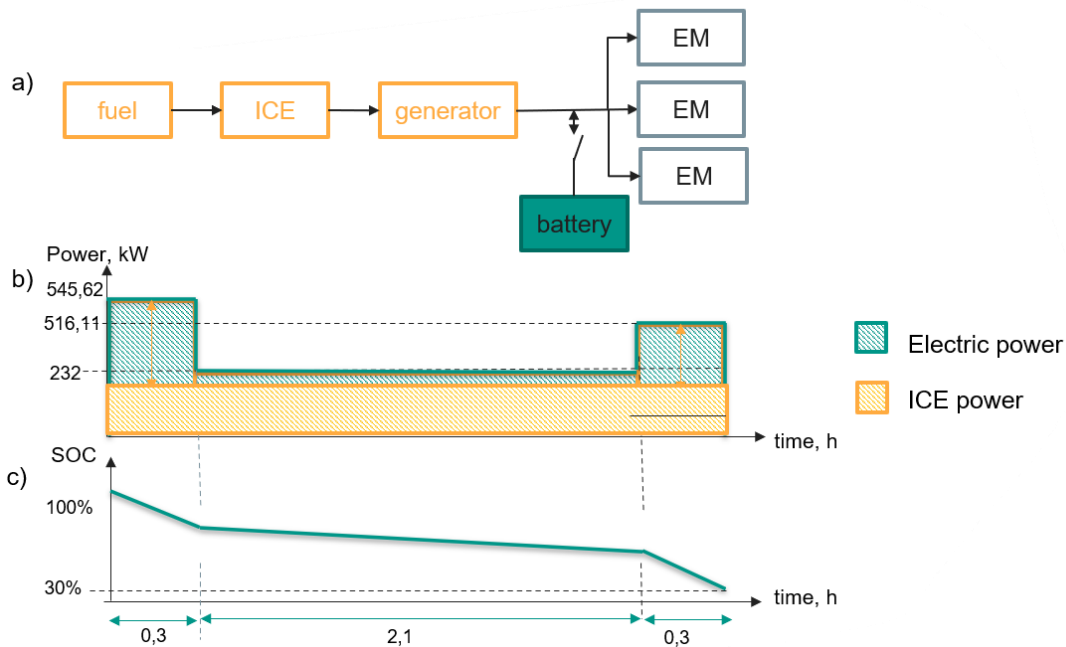


Figure 3.6: Series hybrid propulsion system's a) components connection; b) power distribution graph during full flight mission, kW vs h; c) state of the charge of the battery during the flight

The equation (3.2) for the masses of fuel and battery for the series configurations is modified as followings:

$$m_f = \frac{BSFC}{\eta_{ICE}} \times \alpha P_{cruise} \times t_{total} \quad (3.2)$$

$$m_b = \frac{1}{\eta_{bat}} \left(\frac{(P_{climb} - P_{ICE}) t_{climb} + (P_{cruise} - P_{ICE}) t_{cruise} + (P_{landing} - P_{ICE}) t_{landing}}{e} \right)$$

From the previous figure, 75 percent of the cruise powered by combustion is presented. If the percentage is increased to 100 and 150, the modifications are described in Figures 3.7 and 3.8. This increase can allow for a decrease in the mass of the battery as less power is taken from the electric source. However, such ICE power rise leads to the mass increment of the generator, ICE, and fuel tank as it was described in the previous chapter.

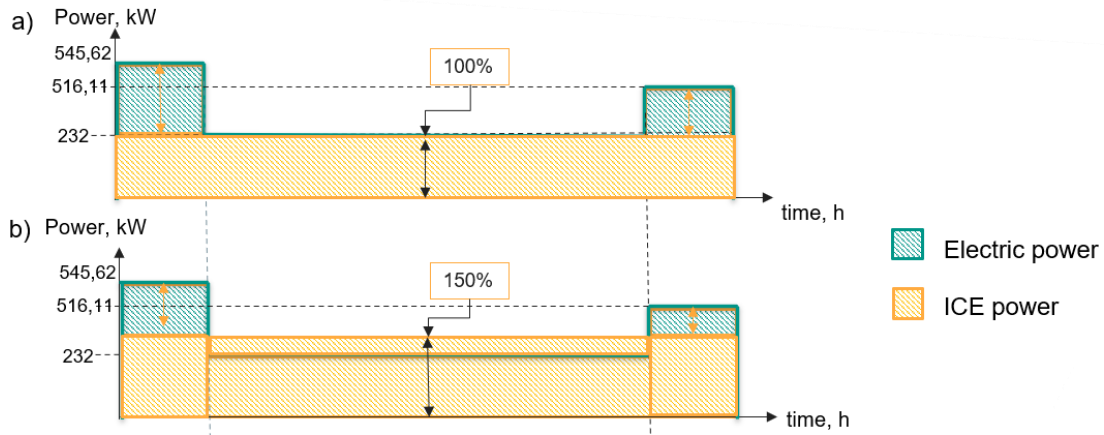


Figure 3.7: Series hybrid propulsion system's power distribution graph for a) 100% and b) 150%, kW vs h;

In terms of the SOC during the increased percentage of fuel consumption above a hundred percent, it is obvious that during the cruise mission, there is no consumption of the battery. For this reason, the graph represents the overall trend of the SOC during the cruise for both cases: 100% and 150% of cruise power in Figure 3.8.

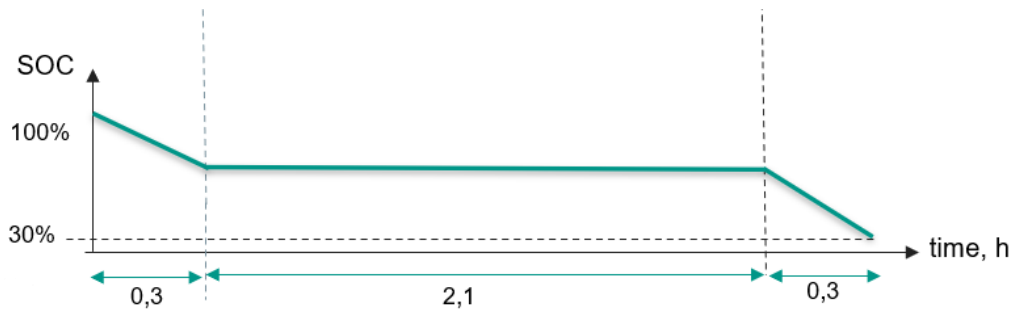


Figure 3.8: Series hybrid propulsion system's state of the charge of the battery for both 100% and 150% of cruise power

By the individual comparison of the weight proportion of elements of the propulsion system among pure ICE, all-electric, and series configurations, it was found that in terms of payload capacity, the pure ICE always has an advantage over others. However, by comparing only series modifications, it is obvious that with the decrease of hybridization ratio, the payload mass will also decrease twice as well as the negative impact of fuel. The numeric values of the components' masses are seen in Figure 3.9 below for $\eta_{bat} = 0.7$. In figure, α means the percentage of cruise power from the combustion.

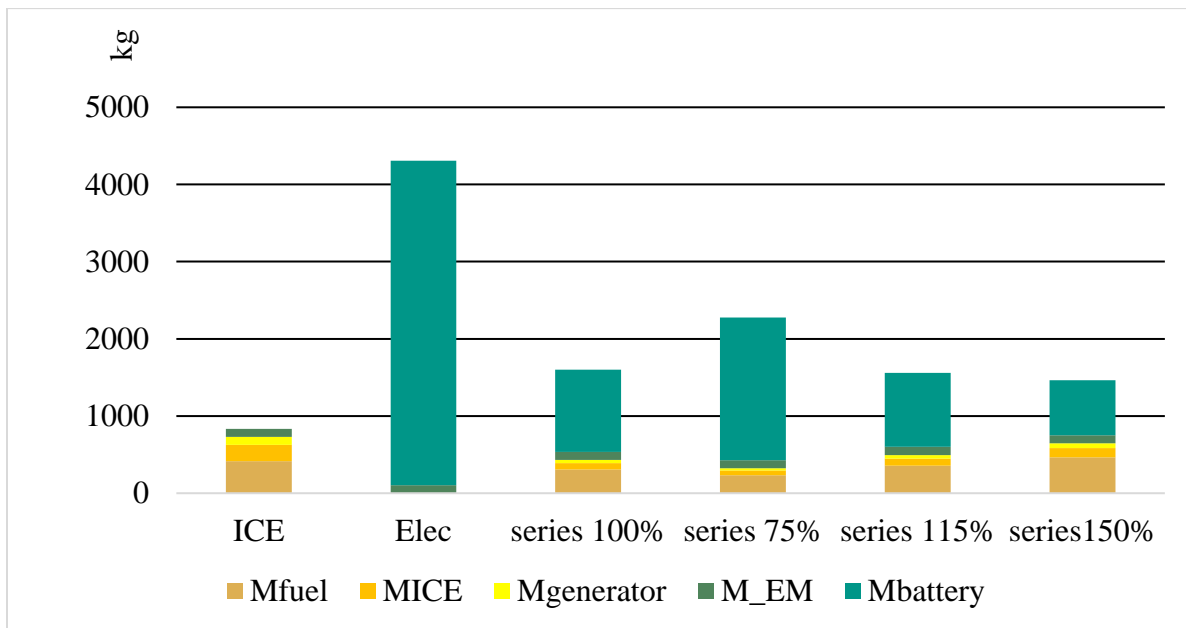


Figure 3.9: Propulsion components mass comparison among pure ICE, all-electric, and series HEPS (varies with α)

Table 3.5: Mass distribution of pure electric, pure fuel, and series HEPS, kg

HEPS configurations	Mfuel	MICE	Mgenerator	M_EM	Mbattery ($\eta_{bat}=0.7$)	Mbattery ($\eta_{bat}=0.5$)	Mtotal
ICE	413,6	212,2	104	104	0	0	834
Elec	0	0	0	104	4202	5883	4306/5987
series 100%	308,6	82	40,2	104	1066	1493	1601/2028
series 75%	231,5	61,4	30,2	104	1850	2590	2277/3017
series 115%	355	94,2	46,2	104	961	1346	1560/1945
series150%	463	122,9	60,2	104	715,3	1000	1465/1750

Mass distribution inside HEPS for $\eta_{bat} = 0.5$ is compared in Table 3.5 above. From the numeric values, it is obvious that the efficiency of the battery significantly influences its weight, and, consequently, the weight of the entire propulsion system. For validation of the results, the 30% of MTOW need to be dedicated to HEPS, which means that HEPS's maximum weight is no more than 1 564.5 kg.

3.2.3. Parallel Hybrid Electric

The next case has components connected to the battery and electric motor parallelly that provides the capability to use the fuel power for charging the battery at the same time as the completion of the cruise mission. Moreover, the charged battery can be consumed for more powerful missions such as the landing or other maneuvers where additional power is needed. The parallel hybrid case also allows to charge the battery either quickly or slowly according to the excess value. For instance, in Figure 3.10c the battery is charging slowly the entire cruise flight, whereas, in Figure 3.11c, it is obvious that the battery has been experiencing fast charging.

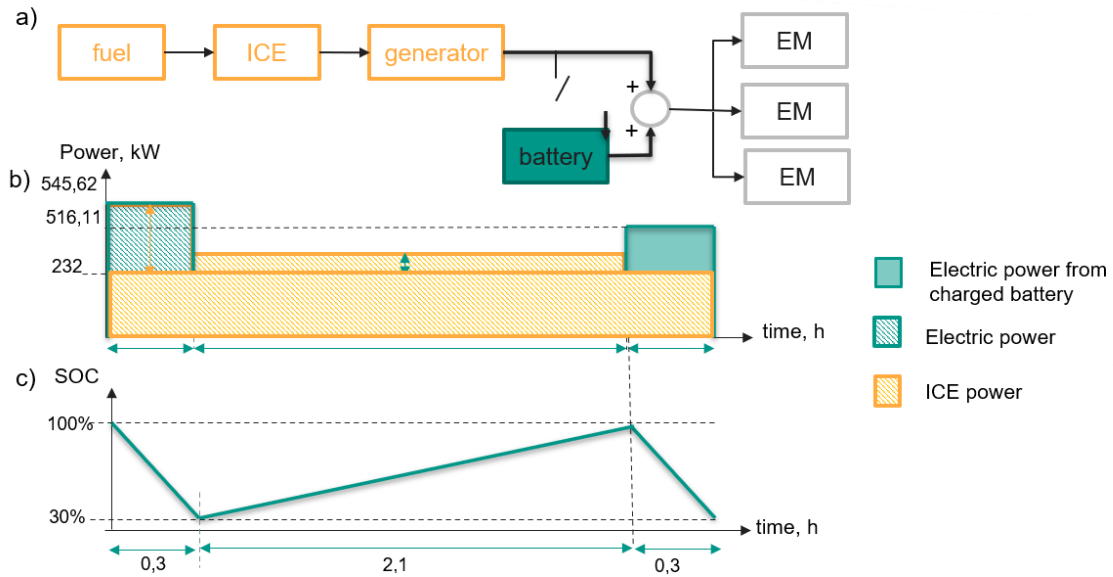


Figure 3.10: Parallel-1 hybrid propulsion system`s a) components connection; b) power distribution graph during full flight mission, kW vs h; c) state of the charge of the battery during the flight

Fast charging has advantages for the parallel hybrid case in that charging can be conducted twice or more as well as the usage of the charged power. This opportunity benefits the weight of HEPS which significantly reduced the weight of the battery and total system compared to the former type (slow charging). This comparison is illustrated in Figure 3.11.

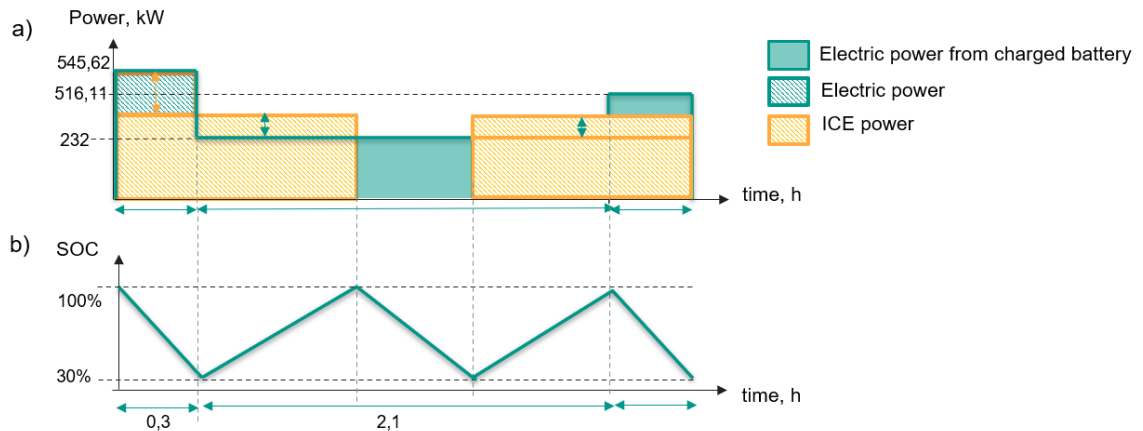


Figure 3.11: Parallel-2 hybrid propulsion system`s a) components connection; b) power distribution graph during full flight mission, kW vs h; c) state of the charge of the battery during the flight

3.2.4. Quiet Takeoff and Landing Scenario

To benefit from silent takeoff and landing, the generated power should be adjusted as shown in Figure 3.12 or 3.13, where the initial and final phases of the mission profile should indeed be completely electrified to decrease HEPS vibration. This flying scenario favors major cities by minimizing noise pollution throughout arrival and departure.

The difference between the two power graphs is in the application of the series or parallel HEPS, where the battery will be charged or not. From the cases described in previous sections, it became clear that the parallel case can satisfy the rechargeability of the battery and its consumption for the landing.

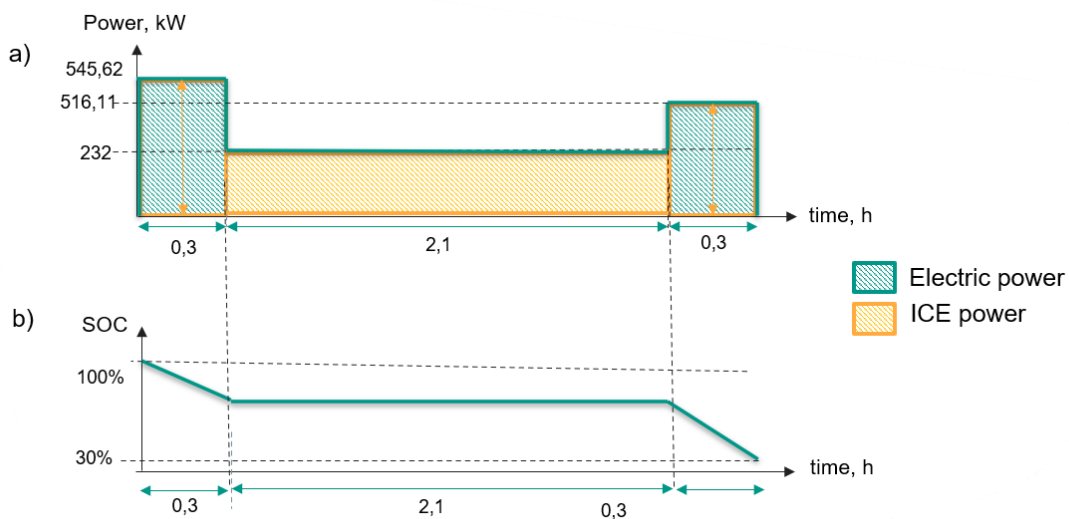


Figure 3.12: Series quiet takeoff and landing system's a) power distribution graph during full flight mission, kW vs h; b) state of the charge of the battery during the flight

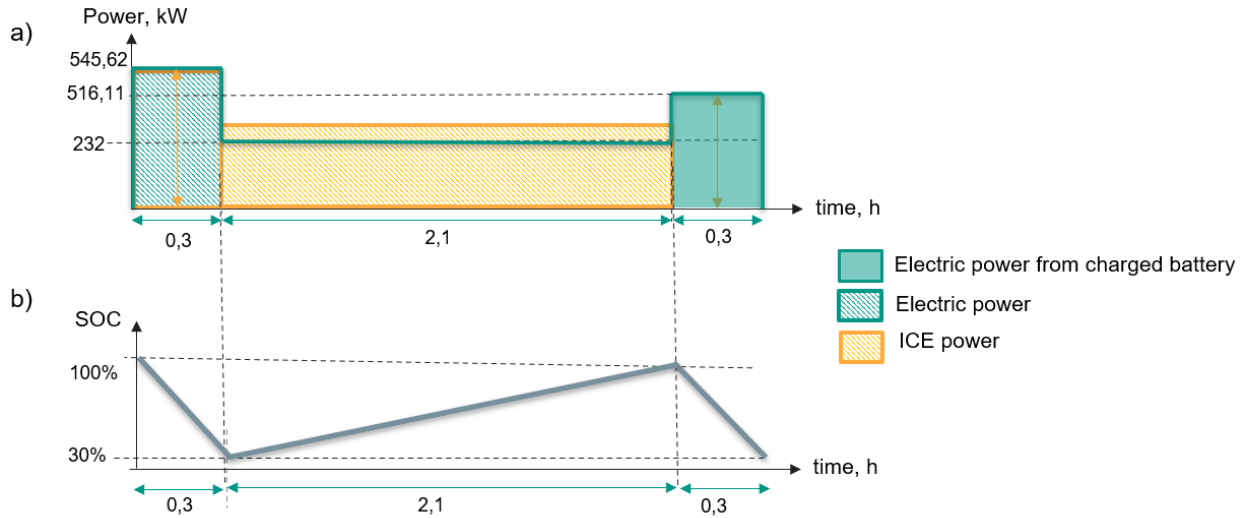


Figure 3.13: Parallel quiet takeoff and landing system`s a) power distribution graph during full flight mission, kW vs h; b) state of the charge of the battery during the flight

By the comparison graph and table, presented in Figure 3.14 and Table 3.6, the parallel HEPS can adequately increase the payload capacity to almost 40% despite series. However, the fuel consumed 34% more than for the series HEPS.

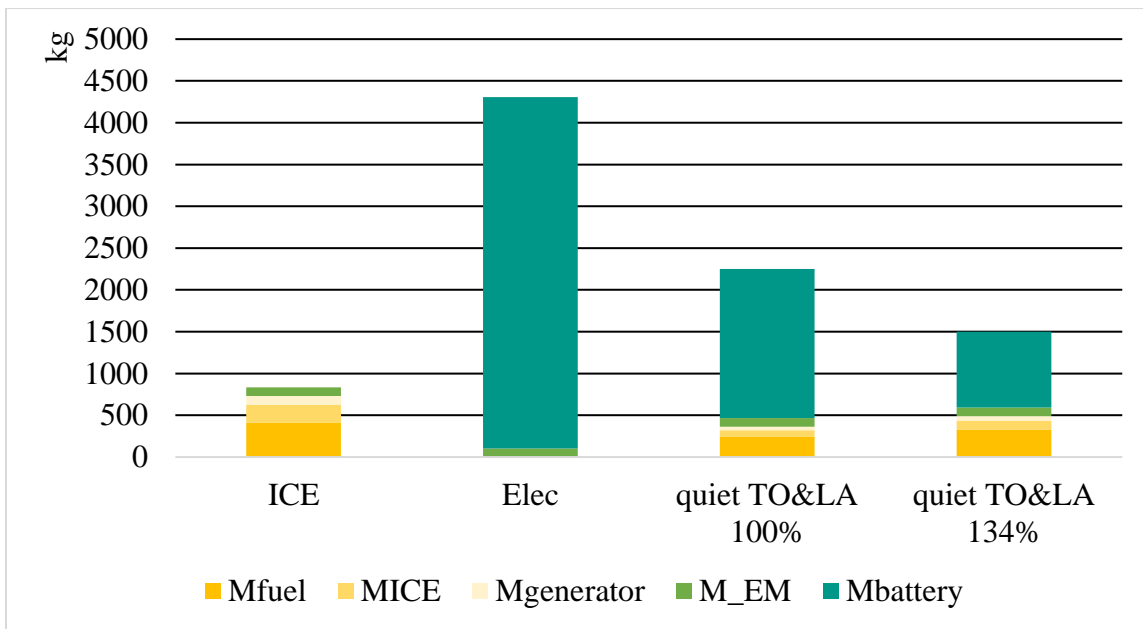


Figure 3.14: Comparison of all-electric, all ICE, series, and parallel quiet takeoff and landing HEPS components mass proportions ($\eta_{bat}=0.7$)

Table 3.6: Mass distribution of all-electric, pure fuel and quiet takeoff and landing HEPS ($\eta_{bat}=0.7$), kg

HEPS configurations	Mfuel	MICE	Mgenerator	M_EM	Mbattery	Mtotal
ICE	413,6	212,2	104	104	0	833,8
Elec	0	0	0	104	4202	4306
quiet TO&LA 100%	240	82	40,2	104	1785	2251,2
quiet TO&LA 134%	325	109,8	53,8	104	909,5	1502,1

Above information is presented for the battery efficiency of 0.7. For the existing battery efficiency, no more than 0.5 is shown Table 3.7 below. Since during the parallel HEPS the battery is charging during the cruise flight, mass of the fuel is now impacted from the efficiency factor of the battery. Time for charging and discharging becomes longer and mass of entire HEP system heavier as more power is needed from the fuel.

Table 3.7: Mass distribution of all-electric, pure fuel and quiet takeoff and landing HEPS ($\eta_{bat}=0.5$), kg

HEPS configurations	Mfuel	MICE	Mgenerator	M_EM	Mbattery	Mtotal
ICE	413,6	212,2	104	104	0	833,5
Elec	0	0	0	104	5883	5987
quiet TO&LA 100%	230	82	40,2	104	2476	2932,2
quiet TO&LA 176.3%	422	144,4	70,75	104	1273	2014,2

3.2.5. Discussion

This section compares all propulsion configurations in terms of their final results in weight distribution. From the obtained results seen in Figure 3.15 and 3.16, it is obvious that the influence of the battery efficiency in comparison of the HEPS is negligible. The comparison presents that the series configurations during hybrid and quiet takeoff and landing interests can significantly reduce the number of emissions as there is a trend in decreased fuel consumption. However, the parallel configuration shows benefits in several terms. Firstly, from the comparison, it seems that the larger increase in the payload is devoted to parallel cases. The reason for that is in reduction of the propulsion weight by up to 20 percent. Next, the parallel HEPS allows researchers to apply aircraft for multiple areas such as the reduction of noise in major cities and for the quiet attack of

the target, which is mostly used in military cases. Moreover, even though the series can reduce CO2 emission at a maximum, the parallel also can deal with the problem in a comparative way having a reduction of almost 15 percent compared to the conventional one. From the attained results, it is obvious that increase of HR reduces the noise and emissions of the aircraft. However, for commercial and heavier airplanes the large HR is not acceptable as there is a low maturity level of battery development.

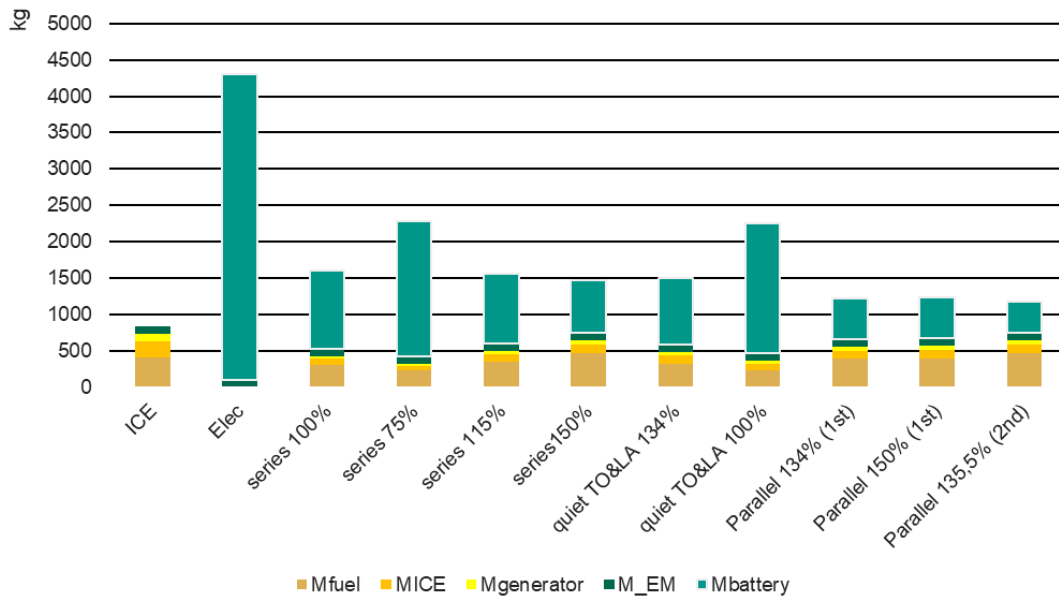


Figure 3.15: Comparison of all researched propulsion systems` mass distribution among components for $\eta_{bat}=0.7$

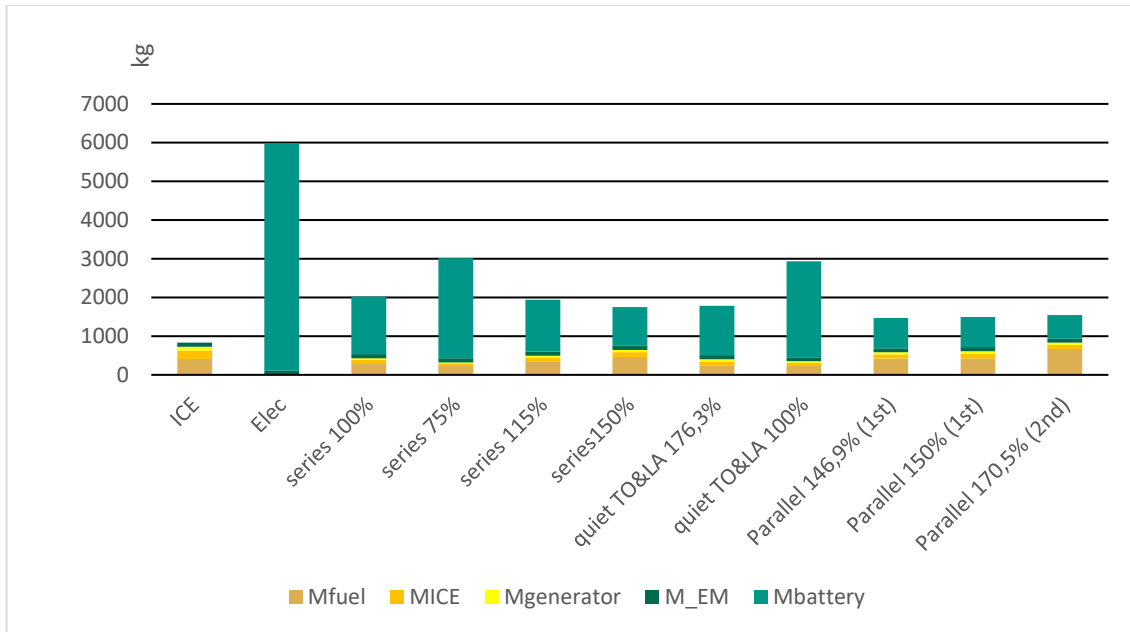


Figure 3.16: Comparison of all researched propulsion systems` mass distribution among components for $\eta_{bat}=0.5$

All the representation of the components` weight influenced by the battery power is illustrated in green, while the combustion components are in yellow. This division of the colors formulate a picture of HEPS components` dependence on the energy types.

Numeric values illustrated in Table 3.8 validates the results of HEPS total weight. The numerical numbers show that the efficiency of the battery has a substantial impact on the amount it weighs thus affecting the mass of the overall propulsion system. In parallel configuration of HEPS, it was found that the battery efficiency has an effect to fuel mass, as more power is needed for charging the battery with less efficiency. With the change of power value from the combustion, the mass of the ICE and generator also changed. During the validation of the findings, where 30% of the MTOW must be allocated to HEPS indicating 1 564.5 kg, it was indicated that improvement of battery characteristics allows the development of HEPS in wider range of aircraft. From the table below fewer HEPS are validated for lower efficiency of the battery ($\eta_{bat}=0.5$). This means that for present battery technologies larger hybridization of the propulsion must be implemented, which cannot deal with the environmental problems as mass of fuel is larger than in the conventional aircraft. The validated HEPS is presented in bold green color, not validated in red.

Table 3.8: Mass distribution of all considered propulsion systems, kg

HEPS configurations	Mfuel	MICE	Mgenerator	M_EM	Mbattery	Mtotal
ICE	413,6	212,2	104	104	0	833,8
<i>for $\eta_{bat}=0.7$</i>						
Elec	0	0	0	104	4202	4306
series 100%	308,6	82	40,2	104	1066	1601
series150%	463	122,9	60,2	104	715,3	1465,4
quiet TO&LA 134%	325	109,8	53,8	104	909,5	1502,1
quiet TO&LA 100%	240	82	40,2	104	1785	2251,2
Parallel 134% (1st)	388,8	109,8	53,8	104	558,5	1214,9
Parallel 135,5% (2nd)	475,24	111	54,39	104	433,85	1178,5
<i>for $\eta_{bat}=0.5$</i>						
Elec	0	0	0	104	5883	5987
series 100%	308,6	82	40,2	104	1493	2027,8
series150%	463	122,9	60,2	104	1000	1750,1
quiet TO&LA 176,3%	422	144,4	70,75	104	1273	2014,2
quiet TO&LA 100%	230	82	40,2	104	2476	2932,2
Parallel 146,9% (1st)	421	120,3	59	104	782	1470,6
Parallel 170,5% (2nd)	665,3	139,7	68,45	104	607	1541,7

Chapter 4 – Conclusion and Future Research Directions

4.1. Conclusion

Because the gains and possible downsides of using HEPS for middle-range aircraft have not been clearly explained, the thesis studied Zunum Aero ZA10 as a reference to gain comparative results. Critically assessing the HEPS for the given sort of airplane, it was found that the most variably applicable propulsion is parallel HEPS. It is characterized by the areas of implementation considered in this research, which are quiet takeoff and landing, hybrid, and quiet attack cases. Even though the parallel HEPS didn't demonstrate almost 45% fuel reduction compared to the conventional as series, it can compete with its wide application and payload capacity. In terms of payload maximization, parallel HEPS could be benefitted by almost 15 percent compared to series. However, the maximum payload capacity is still dedicated to the conventional type. The reason for that is based on the battery characteristics. Even though the thesis has considered the most recent battery type (lithium-ion), it is obvious that the empty weight of electrically powered aircraft remains the almost double weight of conventional aircraft. Thus, decreasing fuel consumption leads to a rapid increase in battery weight and, vice versa, to a decrease in payload mass. This means that increasing the hybridization ratio of middle-range aircraft causes quick growth of its propulsion weight. However, rapid charging of the battery in parallel configuration enables to a reduction of the influence of the hybridization ratio. The reason for that is simply using the recharged battery power. Overall, the development of HEPS is an essential step towards a more sustainable aviation industry.

4.2. Contribution to Knowledge

The project has several achievements and potential contributions to the aviation sector. It provides a comprehensive analysis of the development of a hybrid-electric propulsion system (HEPS) for a medium-range aircraft. It investigates the optimal degree of hybridization required to increase the payload capacity of the aircraft without compromising its range. Assessment of the airframe for the given business aircraft can contribute to the knowledge in the following fields:

- Development of sizing of HEPS.
- Enhancement of the aircraft's initial performance under the considered constraints.

- Acquiring the best ratio of fuel and battery weights for such middle-range aircraft enables us to fulfill the requirement of the constant range and MTOW.
- Comparison of the HEPS performance in the same mission profile and speed parameters.

4.3. Future Research Directions

As the thesis is fully theoretical, for future works, it is obvious that the sizing procedure for HEPS is not expected to be combined with the specification of the actual aircraft design. The reason for that is the need for practical experiences such as testing as there is a need for a more detailed design that evaluates the energy losses, vibration, and cooling systems. Moreover, in the era of fast technology development, research is required to constantly renew and explore, especially in battery and engine exploration. Furthermore, the thesis recommends considering multi-disciplinary optimization of the HEPS which evaluates the energy losses, weight of pipes and converter, and other non-considered small elements such as electric circuits. In addition, the present work can be further applied to other cities and missions. The research has considered only lithium-ion batteries, and other battery types need to be explored. The study has focused on a single case study, thus, the MATLAB code in Appendix can be applied to conduct further research on other aircraft types and models. The study only assesses the benefits of HEPS in terms of reducing the carbon footprint and increasing payload capacity, and other factors such as maintenance costs and safety considerations need to be researched.

References

- [1] NASA. Global Climate Change: Vital Signs of the Planet [Online] Available: <https://climate.nasa.gov/vital-signs/carbon-dioxide/>
- [2] E. A. S. A. (EASA). European Aviation Environmental Report 2019 [Online] Available: https://www.easa.europa.eu/eaer/system/files/usr_uploaded/219473_EASA_EAER_2019_WEB_HI-RES_190311.pdf
- [3] ICAO. "Future of Aviation." <https://www.icao.int/Meetings/FutureOfAviation/Pages/default.aspx>
- [4] M. Lukic, P. Giangrande, A. Hebala, S. Nuzzo, and M. Galea, "Review, Challenges, and Future Developments of Electric Taxiing Systems," *IEEE Transactions on Transportation Electrification*, vol. 5, no. 4, pp. 1441-1457, 2019, doi: 10.1109/TTE.2019.2956862.
- [5] A. Schäfer *et al.*, "Technological, economic and environmental prospects of all-electric aircraft," *Nature Energy*, vol. 4, 02/01 2019, doi: 10.1038/s41560-018-0294-x.
- [6] J. A. Rosero, J. A. Ortega, E. Aldabas, and L. Romeral, "Moving towards a more electric aircraft," *IEEE Aerospace and Electronic Systems Magazine*, vol. 22, no. 3, pp. 3-9, 2007, doi: 10.1109/MAES.2007.340500.
- [7] W. Cao, B. C. Mecrow, G. J. Atkinson, J. W. Bennett, and D. J. Atkinson, "Overview of Electric Motor Technologies Used for More Electric Aircraft (MEA)," *IEEE Transactions on Industrial Electronics*, vol. 59, no. 9, pp. 3523-3531, 2012, doi: 10.1109/TIE.2011.2165453.
- [8] O. Bottauscio, G. Serra, M. Zucca, and M. Chiampi, "Role of Magnetic Materials in a Novel Electrical Motogenerator for the More Electric Aircraft," *IEEE Transactions on Magnetics*, vol. 50, no. 4, pp. 1-4, 2014, doi: 10.1109/TMAG.2013.2284937.
- [9] J. Serafini, M. Cremaschini, G. Bernardini, L. Solero, C. Ficuciello, and M. Gennaretti, "Conceptual All-Electric Retrofit of Helicopters: Review, Technological Outlook, and a Sample Design," *IEEE Transactions on Transportation Electrification*, vol. 5, no. 3, pp. 782-794, 2019, doi: 10.1109/TTE.2019.2919893.
- [10] F. Kelch, Y. Yang, B. Bilgin, and A. emadi, "Investigation and design of an axial flux permanent magnet machine for a commercial midsize aircraft electric taxiing system," *IET Electrical Systems in Transportation*, vol. 8, 07/26 2017, doi: 10.1049/iet-est.2017.0039.
- [11] *Aircraft Electrical Propulsion – Onwards and Upwards*: Poland Berger, 2018.
- [12] J. Benzaquen, J. He, and B. Mirafzal, "Toward more electric powertrains in aircraft: Technical challenges and advancements," *CES Transactions on Electrical Machines and Systems*, vol. 5, no. 3, pp. 177-193, 2021, doi: 10.30941/CESTEMS.2021.00022.
- [13] A. Adib *et al.*, "E-Mobility — Advancements and Challenges," *IEEE Access*, vol. 7, pp. 165226-165240, 2019, doi: 10.1109/ACCESS.2019.2953021.
- [14] M. Phattanasak, R. Gavagsaz-Ghoachani, J. P. Martin, B. Nahid-Mobarakeh, S. Pierfederici, and B. Davat, "Control of a Hybrid Energy Source Comprising a Fuel Cell and Two Storage Devices Using Isolated Three-Port Bidirectional DC–DC Converters," *IEEE Transactions on Industry Applications*, vol. 51, no. 1, pp. 491-497, 2015, doi: 10.1109/TIA.2014.2336975.
- [15] N. Swaminathan and Y. Cao, "An Overview of High-Conversion High-Voltage DC–DC Converters for Electrified Aviation Power Distribution System," *IEEE Transactions on*

- Transportation Electrification*, vol. 6, no. 4, pp. 1740-1754, 2020, doi: 10.1109/TTE.2020.3009152.
- [16] C. Ivey, A. Alfares, and J. He, "Hybrid-Electric Aircraft Propulsion Drive Based on SiC Triple Active Bridge Converter," in *2021 IEEE/IAS Industrial and Commercial Power System Asia (I&CPS Asia)*, 18-21 July 2021 2021, pp. 431-436, doi: 10.1109/ICPSAsia52756.2021.9621503.
- [17] J. R. Serrano, A. O. Tiseira, L. M. García-Cuevas, and P. Varela, "Computational Study of the Propeller Position Effects in Wing-Mounted, Distributed Electric Propulsion with Boundary Layer Ingestion in a 25 kg Remotely Piloted Aircraft," *Drones*, vol. 5, no. 3, doi: 10.3390/drones5030056.
- [18] H. D. Kim, A. T. Perry, and P. J. Ansell, "A Review of Distributed Electric Propulsion Concepts for Air Vehicle Technology," in *2018 AIAA/IEEE Electric Aircraft Technologies Symposium*, (AIAA Propulsion and Energy Forum: American Institute of Aeronautics and Astronautics, 2018.
- [19] B. A. Adu-Gyamfi and C. Good, "Electric aviation: A review of concepts and enabling technologies," *Transportation Engineering*, vol. 9, p. 100134, 2022/09/01/ 2022, doi: <https://doi.org/10.1016/j.treng.2022.100134>.
- [20] S. Sahoo, X. Zhao, and K. Kyprianidis, "A Review of Concepts, Benefits, and Challenges for Future Electrical Propulsion-Based Aircraft," *Aerospace*, vol. 7, no. 4, doi: 10.3390/aerospace7040044.
- [21] D. P. Decerio and D. K. Hall, "Benefits of Parallel Hybrid Electric Propulsion for Transport Aircraft," *IEEE Transactions on Transportation Electrification*, vol. 8, no. 4, pp. 4054-4066, 2022, doi: 10.1109/TTE.2022.3193622.
- [22] M. A. Rendón, C. D. Sánchez R, J. Gallo M, and A. H. Anzai, "Aircraft Hybrid-Electric Propulsion: Development Trends, Challenges and Opportunities," *Journal of Control, Automation and Electrical Systems*, vol. 32, no. 5, pp. 1244-1268, 2021/10/01 2021, doi: 10.1007/s40313-021-00740-x.
- [23] C. Friedrich and P. Robertson, *Hybrid-Electric Propulsion Systems for Aircraft*. 2013.
- [24] A. Lentsch. "Diamond Aircraft proudly presents the world's first serial hybrid electric aircraft "DA36 E-Star"." <https://www.diamondaircraft.com/en/about-diamond/newsroom/news/article/diamond-aircraft-proudly-presents-the-worlds-first-serial-hybrid-electric-aircraft-da36-e-star/>.
- [25] B. Schiff. "AMPAIRE 337 'PARALLEL HYBRID' UNVEILED." <https://www.aopa.org/news-and-media/all-news/2019/june/10/ampaire-337-parallel-hybrid-unveiled>
- [26] B. Sampson. "Rolls-Royce tests hybrid aero propulsion system." <https://www.aerospacetestinginternational.com/news/electric-hybrid/rolls-royce-tests-hybrid-aero-propulsion-system.html>
- [27] A. S. Saeed, A. B. Younes, C. Cai, and G. Cai, "A survey of hybrid Unmanned Aerial Vehicles," *Progress in Aerospace Sciences*, vol. 98, pp. 91-105, 2018/04/01/ 2018, doi: <https://doi.org/10.1016/j.paerosci.2018.03.007>.
- [28] B. J. Brelje and J. R. R. A. Martins, "Electric, hybrid, and turboelectric fixed-wing aircraft: A review of concepts, models, and design approaches," *Progress in Aerospace Sciences*, vol. 104, pp. 1-19, 2019/01/01/ 2019, doi: <https://doi.org/10.1016/j.paerosci.2018.06.004>.

- [29] T. Dean, G. Wroblewski, and P. Ansell, "Mission Analysis and Component-Level Sensitivity Study of Hybrid-Electric General-Aviation Propulsion Systems," *Journal of Aircraft*, vol. 55, pp. 1-12, 09/20 2018, doi: 10.2514/1.C034635.
- [30] M. Voskuijl, J. van Bogaert, and A. G. Rao, "Analysis and design of hybrid electric regional turboprop aircraft," *CEAS Aeronautical Journal*, vol. 9, no. 1, pp. 15-25, 2018/03/01 2018, doi: 10.1007/s13272-017-0272-1.
- [31] G. E. Wroblewski and P. J. Ansell, "Mission Analysis and Emissions for Conventional and Hybrid-Electric Commercial Transport Aircraft," *Journal of Aircraft*, vol. 56, no. 3, pp. 1200-1213, 2019/05/01 2019, doi: 10.2514/1.C035070.
- [32] R. de Vries, M. F. M. Hoogreef, and R. Vos, "Range Equation for Hybrid-Electric Aircraft with Constant Power Split," *Journal of Aircraft*, vol. 57, no. 3, pp. 552-557, 2020/05/01 2020, doi: 10.2514/1.C035734.
- [33] B. Yang, F. Lou, and N. L. Key, "Conceptual Design of a 10-passenger Thin-haul Electric Aircraft," in *2020 AIAA/IEEE Electric Aircraft Technologies Symposium (EATS)*, 26-28 Aug. 2020 2020, pp. 1-18.
- [34] P. G. Juretzko, M. Immer, and J. Wildi, "Performance analysis of a hybrid-electric retrofit of a RUAG Dornier Do 228NG," *CEAS Aeronautical Journal*, vol. 11, no. 1, pp. 263-275, 2020/01/01 2020, doi: 10.1007/s13272-019-00420-2.
- [35] Y. Liu, H. Wang, J. Zhang, T. Jiang, and Y. Zheng, "Retrofit and New Design of Regional Aircraft with Hybrid Electric Propulsion," in *2021 AIAA/IEEE Electric Aircraft Technologies Symposium (EATS)*, 11-13 Aug. 2021 2021, pp. 1-12, doi: 10.23919/EATS52162.2021.9704854.
- [36] C. Pernet *et al.*, "Methodology for Sizing and Performance Assessment of Hybrid Energy Aircraft," *Journal of Aircraft*, vol. 52, no. 1, pp. 341-352, 2015/01/01 2014, doi: 10.2514/1.C032716.
- [37] R. Glasscock, M. Galea, W. Williams, and T. Glesk, "Hybrid Electric Aircraft Propulsion Case Study for Skydiving Mission," *Aerospace*, vol. 4, no. 3, doi: 10.3390/aerospace4030045.
- [38] R. de Vries, M. Brown, and R. Vos, "Preliminary Sizing Method for Hybrid-Electric Distributed-Propulsion Aircraft," *Journal of Aircraft*, vol. 56, no. 6, pp. 2172-2188, 2019/11/01 2019, doi: 10.2514/1.C035388.
- [39] C. E. D. Riboldi, "An optimal approach to the preliminary design of small hybrid-electric aircraft," *Aerospace Science and Technology*, vol. 81, pp. 14-31, 2018/10/01/ 2018, doi: <https://doi.org/10.1016/j.ast.2018.07.042>.
- [40] Y. Xie, A. Savvarisal, A. Tsourdos, D. Zhang, and J. Gu, "Review of hybrid electric powered aircraft, its conceptual design and energy management methodologies," *Chinese Journal of Aeronautics*, vol. 34, no. 4, pp. 432-450, 2021/04/01/ 2021, doi: <https://doi.org/10.1016/j.cja.2020.07.017>.
- [41] E. Fornaro, M. Cardone, and A. Dannier, "A Comparative Assessment of Hybrid Parallel, Series, and Full-Electric Propulsion Systems for Aircraft Application," *IEEE Access*, vol. 10, pp. 28808-28820, 2022, doi: 10.1109/ACCESS.2022.3158372.
- [42] D. Sziroczak, I. Jankovics, I. Gal, and D. Rohacs, "Conceptual design of small aircraft with hybrid-electric propulsion systems," *Energy*, vol. 204, p. 117937, 2020/08/01/ 2020, doi: <https://doi.org/10.1016/j.energy.2020.117937>.

- [43] M. Pettes-Duler, X. Roboam, B. Sareni, Y. Lefevre, J.-F. Llibre, and M. Fénot, "Multidisciplinary Design Optimization of the Actuation System of a Hybrid Electric Aircraft Powertrain," *Electronics*, vol. 10, no. 11, doi: 10.3390/electronics10111297.
- [44] E. National Academies of Sciences and Medicine, *Commercial Aircraft Propulsion and Energy Systems Research: Reducing Global Carbon Emissions*. Washington, DC: The National Academies Press (in English), 2016, p. 122.
- [45] A. Misra, "Energy Storage for Electrified Aircraft: The Need for Better Batteries, Fuel Cells, and Supercapacitors," *IEEE Electrification Magazine*, vol. 6, no. 3, pp. 54-61, 2018, doi: 10.1109/MELE.2018.2849922.
- [46] T. C. Cano *et al.*, "Future of Electrical Aircraft Energy Power Systems: An Architecture Review," *IEEE Transactions on Transportation Electrification*, vol. 7, no. 3, pp. 1915-1929, 2021, doi: 10.1109/TTE.2021.3052106.
- [47] J. Harikumaran *et al.*, "Failure Modes and Reliability Oriented System Design for Aerospace Power Electronic Converters," *IEEE Open Journal of the Industrial Electronics Society*, vol. 2, pp. 53-64, 2021, doi: 10.1109/OJIES.2020.3047201.
- [48] M. S. S. Ignacio Echavarria Diaz-Guardamino, Martin Nuesseler, "Challenges associated to high power Hybrid Electric Propulsion in Aerospace."
- [49] Q. Zhu, A. Forsyth, and R. Todd, "Investigation of Hybrid Electric Aircraft Operation on Battery Degradation," in *2018 IEEE International Conference on Electrical Systems for Aircraft, Railway, Ship Propulsion and Road Vehicles & International Transportation Electrification Conference (ESARS-ITEC)*, 7-9 Nov. 2018 2018, pp. 1-6, doi: 10.1109/ESARS-ITEC.2018.8607617.
- [50] J. G. Leishman, "Flight Range & Endurance," *Introduction to Aerospace Flight Vehicles* Embry-Riddle Aeronautical University, 2022.
- [51] D. Finger, C. Braun, and C. Bil, *An Initial Sizing Methodology for Hybrid-Electric Light Aircraft*. 2018.
- [52] F. Zhang *et al.*, "Comparative study of energy management in parallel hybrid electric vehicles considering battery ageing," *Energy*, vol. 264, p. 123219, 2023/02/01/ 2023, doi: <https://doi.org/10.1016/j.energy.2022.123219>.
- [53] M. Kozlova, T. Nykänen, and J. S. Yeomans, "Technical Advances in Aviation Electrification: Enhancing Strategic R&D Investment Analysis through Simulation Decomposition," *Sustainability*, vol. 14, no. 1, doi: 10.3390/su14010414.
- [54] M. Factory. Zunum Aero ZA10: Hybrid-Electric Regional Airliner Aircraft [2022] [Online] Available: https://www.militaryfactory.com/aircraft/detail.php?aircraft_id=2028

Appendix MATLAB Code

```

% aircraft specifications input data
MTOW=51250;           %Maximum Takeoff Weight
Wfuel=3630;          %mass of fuel
s=16;                %span
c=1.444;             %chord
AR=s/c;              %Aspect ratio
WingArea=s^2/AR;     %Wing area S
Vendurance=116.779; %Velocity for maximum endurance
Vmax=151.76;         %Maximum cruise velocity
Vrange=142;          %Velocity for maximum range
RC=8.13;             %Rate of climb
H=7620;              %cruise altitude
rosl=1.225;          %air density at the ground
beta=1/9042;         % beta for calculation of air density at the cruise altitude
roH=rosl*exp(-H*beta); %air density at the cruise altitude
e=0.7;               %coefficient
k=1/(e*pi*AR);       %value dependant on induced drag
qinf=roH*Vrange^2 / 2; %dynamic pressure
cl=(MTOW-Wfuel/2) / (qinf*WingArea); %coefficient of lift calculation
cdmin=(4*(MTOW-Wfuel/2)^2*k) / (roH^2*WingArea^2*Vmax^4); %coefficient of drag minimum calculation
Vcheckendurance=sqrt((2*(MTOW-Wfuel/2))/(roH*WingArea) * (sqrt(k/(3*cdmin)))); %check the velocity for maximum endurance
cd=cdmin + k*cl^2; %calculate coefficient of drag
T=qinf*WingArea*cd; %evaluate Thrust force
Range=1126540;       %Range of the aircraft
Vclimb=Vendurance;

%power distribution among full mission profile
Pr=T*Vrange; %required power for cruise
Pexcessclimb= MTOW*RC; %excess power during climbing
Pexcesslanding=(MTOW-Wfuel)*RC; %excess power during landing
Pclimb=1/2 * roH*Vclimb^3*WingArea*cd + Pexcessclimb; %total power for climbing
Planding = 1/2 * roH*Vclimb^3*WingArea*cd + Pexcesslanding; %total power for landing
Pcruise=Pr; %power for cruise is equal to required power

% full mission profile time
%all time values are transferred to h
tclimb=18/60; %time for climbing and landing is equal
tcruise=Range/(Vendurance*3600) - 2*tclimb; % time for cruise is calculated by the given equation
tlanding=tclimb;
t_total=tclimb+tcruise+tlanding; %total mission profile time

%input data for elements`mass distribution calculation
BSE=250; %specific energy of the battery in W/kg unit
BSFC=225/1000; %Brake Specific Fuel Coefficient is transferred g to kg
%HEPS components`efficiencies for ICE, generator and EM
nICE=0.4;
ngen=0.98;
nEM=0.98;
%Specific powers of HEPS components
PstarICE=1000;
Pstangen=5000;
Pstarem=5000;

```

```

%starting calculation of mass distribution for different configurations

%for pure ICE

mfuel_ICE=(BSFC/nICE) *(Pclimb*tclimb+Pcruise*tcruise+Planding*tlanding)/1000; %mass of fuel
mICE_ICE=Pclimb / PstarICE*nICE; %mass of ICE
mgen_ICE= Pclimb / Pstargen*nngen; %mass of generator
mEM_ICE=Pclimb/Pstarem*nEM; %mass of EM
m_ICE_total=mfuel_ICE+mICE_ICE+mgen_ICE+mEM_ICE; %total mass of propulsion system

% for pure EM
Cb_EM=1/0.7 * (Pclimb*tclimb + Pcruise*tcruise + Planding*tlanding); %Capacity of the battery
mb_EM=Cb_EM/BSE; %mass of battery
mEM_EM = Pclimb/Pstarem*nEM; %mass of EM
m_EM_total=mb_EM+mEM_EM; %total mass of propulsion system

%for series HEPS

%mfuel part describes the dependance of the components weight to the proportion of fueled power
PICE=Pcruise;
mfuel_series=BSFC/nICE * PICE/1000 * t_total;
mICE_series=PICE / PstarICE*nICE;
mgen_series=PICE/Pstargen*nngen;

%electric part illustrates the dependance of the components weight to the proportion of electrified power
Pexcessclimb=Pclimb-Pcruise;
Pexcesslanding=Planding-Pcruise;
Cb_hybrid=1/0.7 * (Pexcessclimb*tclimb + Pexcesslanding*tlanding);
mb_hybrid=Cb_hybrid/BSE;
mEM_hybrid = Pclimb/Pstarem*nEM;
m_hybrid_total=mfuel_series+mICE_series+mgen_series+mb_hybrid+mEM_hybrid;

%for series HEPS of 75% of cruise ICE, where alpha is 0.75
%fuel part
PICE_75=0.75*Pr;
mfuel_series75=BSFC/nICE * PICE_75/1000 * t_total;
mICE_series75=PICE_75 / PstarICE*nICE;
mgen_series75=PICE_75/Pstargen*nngen;
%electric part
mEM_series75=mEM_EM;
Cb_series75=1/0.7 * ((Pclimb-PICE_75)*tclimb +(Pcruise-PICE_75)*tcruise + (Planding-PICE_75)*tlanding);
mb_series75=Cb_series75/BSE;
m_hybrid75_total=mfuel_series75+mb_series75+mEM_series75+mgen_series75+mICE_series75;

```

By the change of the alpha, the HR will be changed that has a relationship to masses of generator, ICE, battery and fuel. Previously, HR is increased, next codes demonstrates its decrease, where $\alpha > 1.0$

```

%for series HEPS of 115% of cruise ICE, where alpha is 1.15
%fuel part
PICE_115=1.15*Pr;
mfuel_series115=BSFC/nICE * PICE_115/1000 * t_total;
mICE_series115=PICE_115 / PstarICE*nICE;
mgen_series115=PICE_115/Pstargen*ngen;
%electric part
mEM_series115=mEM_EM;
Cb_series115=1/0.7 * ((Pclimb-PICE_115)*tclimb + (Planding-PICE_115)*tlanding);
mb_series115=Cb_series115/BSE;
m_hybrid115_total=mfuel_series115+mb_series115+mEM_series115+mgen_series115+mICE_series115;

%for series HEPS of 125% of cruise ICE, where alpha is 1.25
%fuel part
PICE_125=1.25*Pr;
mfuel_series125=BSFC/nICE * PICE_125/1000 * t_total;
mICE_series125=PICE_125 / PstarICE*nICE;
mgen_series125=PICE_125/Pstargen*ngen;
%electric part
mEM_series125=mEM_EM;
Cb_series125=1/0.7 * ((Pclimb-PICE_125)*tclimb + (Planding-PICE_125)*tlanding);
mb_series125=Cb_series125/BSE;
m_hybrid125_total=mfuel_series125+mb_series125+mEM_series125+mgen_series125+mICE_series125;

```

Parallel onfiguration:

```
%parallel case 1 (charged only once)
%parallel HEPS for alpha=1.34

alpha=1.34;
PICE_parallel1=alpha*Pcruise;
mEM_parallel1=mEM_EM;
Cb_parallel1=1/0.7 * ((Pclimb-Pcruise)*tclimb);
tcharg=Cb_parallel1/(ngen*(PICE_parallel1-Pcruise));
mb_parallel1=Cb_parallel1/BSE;
mfuel_parallel1=BSFC/nICE * ((PICE_parallel1/1000 * tcharg) + (Pcruise/1000 *(t_total-tcharg)));
mICE_parallel1=PICE_parallel1/ PstarICE*nICE;
mgen_parallel1=PICE_parallel1/Pstargen*ngen;
m_parallel1_total=mfuel_parallel1+mb_parallel1+mEM_parallel1+mgen_parallel1+mICE_parallel1;

%parallel HEPS for apha=1.5

alpha2=1.67;
PICE_parallel2=alpha2*Pcruise;
mEM_parallel2=mEM_EM;
Cb_parallel2=1/0.7 * ((Pclimb-Pcruise)*tclimb);
tcharg2=Cb_parallel2/(ngen*(PICE_parallel2-Pcruise));
mb_parallel2=Cb_parallel2/BSE;
mfuel_parallel2=BSFC/nICE * ((PICE_parallel2/1000 * tcharg2) + (Pcruise/1000 *(t_total-tcharg2)));
mICE_parallel2=PICE_parallel2/ PstarICE*nICE;
mgen_parallel2=PICE_parallel2/Pstargen*ngen;
m_parallel2_total=mfuel_parallel2+mb_parallel2+mEM_parallel2+mgen_parallel2+mICE_parallel2;

%parallel case 2 (charged twice or more)
%parallel HEPS for apha=2.01

alpha3=1.355;
PICE_parallel3=alpha3*Pcruise;
mEM_parallel3=mEM_EM;
Cb_parallel3=1/0.7 * ((Pclimb-PICE_parallel3)*tclimb);
tcharg3=Cb_parallel3/(ngen*(PICE_parallel3-Pcruise));
tdischarg3=Cb_parallel3/(nEM*Pcruise);
mb_parallel3=Cb_parallel3/BSE;
mfuel_parallel3=BSFC/nICE * ((PICE_parallel3/1000 * 2*tcharg3));
mICE_parallel3=PICE_parallel3/ PstarICE*nICE;
mgen_parallel3=PICE_parallel3/Pstargen*ngen;
m_parallel3_total=mfuel_parallel3+mb_parallel3+mEM_parallel3+mgen_parallel3+mICE_parallel3;
```

For quiet takeoff and landing interest:

```
%for quiet TO & L of 100% of cruise ICE
%fuel part
PICE=Pr;
mfuel_quietTO=BSFC/nICE * PICE/1000 * tcruise;
mICE_quietTO=PICE/ PstarICE*nICE;
mgen_quietTO=PICE/Pstargen*ngen;
%electric part
mEM_quietTO=mEM_EM;
Cb_quietTO=1/0.7 * (Pclimb*tclimb + Planding*tlanding);
mb_quietTO=Cb_quietTO/BSE;
m_quietTO_total=mfuel_quietTO+mb_quietTO+mEM_quietTO+mgen_quietTO+mICE_quietTO;

%for quite TO and Landing of 134% cruise power
%fuel part
PICE_quiteTO_115=1.34*Pr;
mfuel_quiteTO_115=BSFC/nICE * PICE_quiteTO_115/1000 * tcruise + BSFC/nICE * Pcruise/1000 * (tcruise-tchang);
mICE_quiteTO_115=PICE_quiteTO_115 / PstarICE*nICE;
mgen_quiteTO_115=PICE_quiteTO_115/Pstargen*ngen;
%electric part
mEM_quiteTO_115=mEM_EM;
Cb_quiteTO_115=1/0.7 * (Pclimb*tclimb);
mb_quiteTO_115=Cb_quiteTO_115/BSE;
m_quiteTO_115_total=mfuel_quiteTO_115+mb_quiteTO_115+mEM_quiteTO_115+mgen_quiteTO_115+mICE_quiteTO_115;
```